SAE TECHNICAL PAPER SERIES

2006-01-3652

Investigation of Intake Concepts for a Formula SAE Four-Cylinder Engine Using 1D/3D (Ricardo WAVE-VECTIS) Coupled Modeling Techniques

Mark Claywell, Donald Horkheimer and Garrett Stockburger
University of Minnesota – Twin Cities

Motorsports Engineering Conference & Exhibition
Dearborn, Michigan
December 5-7, 2006

SAE International™

400 Commonwealth Drive, Warrendale, PA 15096-0001 U.S.A. Tel: (724) 776-4841 Fax: (724) 776-0790 Web: www.sae.org

The Engineering Meetings Board has approved this paper for publication. It has successfully completed SAE's peer review process under the supervision of the session organizer. This process requires a minimum of three (3) reviews by industry experts.

For permission and licensing requests contact:

SAE Permissions
400 Commonwealth Drive
Warrendale, PA 15096-0001-USA
Email: permissions@sae.org
Tel: 724-772-4028
Fax: 724-776-3036

SAE® Global Mobility Database®

All SAE papers, standards, and selected books are abstracted and indexed in the Global Mobility Database.

For multiple print copies contact:

SAE Customer Service
Tel: 877-606-7323 (inside USA and Canada)
Tel: 724-776-4970 (outside USA)
Fax: 724-776-0790
Email: CustomerService@sae.org

ISSN 0148-7191

Printed in USA

2006-01-3652

Investigation of Intake Concepts for a Formula SAE Four-Cylinder Engine Using 1D/3D (Ricardo WAVE-VECTIS) Coupled Modeling Techniques

Mark Claywell, Donald Horkheimer and Garrett Stockburger
University of Minnesota – Twin Cities

ABSTRACT

Many variations of intake designs currently exist in Formula SAE. This paper sets out to investigate if one intake design provides improved performance over another and to gain further insight into the nature of the airflow within a Formula SAE intake.

Intake designs are first classified by physical layout. Then Ricardo's software WAVE (1D) and VECTIS (3D) are used to investigate the performance of the three most common intake concepts as well as two variations of the base concepts for a naturally aspirated four-cylinder Formula SAE engine. Each intake concept is modeled across an RPM range using a WAVE simulation. Simulations are performed at three different RPM using WAVE and VECTIS coupled at the intake inlet and runner exits of each intake concept. A 3D simplified CAD geometry of each intake is used for the VECTIS part of the simulation. An unsteady flow analysis was used instead of a steady flow analysis due to the nature of the flow within an engine.

Simplifying assumptions and the use of computational grid convergence analysis and the comparison of 1D and 1D/3D simulations are described. Evaluations of intake performance are also discussed. Intake performance is determined by several factors: cylinder-to-cylinder volumetric efficiency, time of choked flow in the restrictor, total pressure loss along the restrictor, sound spectrum frequency content, and physical packaging characteristics. In addition, intake manifold and restrictor interaction is discussed as well as visualization of adverse flow conditions. Packaging considerations such as the location of flow bends for minimum pressure loss are also discussed.

The authors found that what they define as the Conical-Spline Intake Concept offers the best performance. This intake concept offers an order of magnitude improvement in the variation of cylinder-to-cylinder volumetric efficiency with consequent improvements in ease of tuning and acoustic noise emission control. In addition, it has the lowest total pressure drop along the diffuser of all the concepts evaluated.

INTRODUCTION

Formula SAE is a student collegiate design series devoted to the design and construction of open-wheeled race cars. Over 200 schools participate in this series with competitive events held in the United States of America, the United Kingdom, Germany, Italy, Brazil, Japan, and Australia. These events are known for the enthusiastic participation of student engineers and the wide range of engineering ideas and innovations utilized on the cars.

The governing rules contain a limited number of technical regulations that constrain the students' design choices, leaving a large design space to explore. Although many other avenues of exploration in engine package design exist, a large majority of teams use a naturally-aspirated four-cylinder engine derived from available motorcycles. A team's engine choice is limited to any four-stroke with a displacement less than 610 cc. The number of cylinders is unlimited. Rules also require a 20-mm air restrictor when 94 or 100 Octane fuel is used and a 19-mm air restrictor when E-85 fuel is used.

With four-cylinder Formula SAE engines, the shape, layout, size, and packaging of intake manifolds vary. Each team uses different runner lengths, plenum volumes, restrictor designs, etc for its intake design. In addition to a variety of intake designs there are different exhaust configurations that make direct comparisons difficult. Individual team's choices when it comes to intake and exhaust configurations are driven by the team's expertise and performance goals. While intake concepts vary, they can be classified. A broad range of intakes from many teams were evaluated and placed in several groups.

The four most prevalent designs found at the Formula SAE competition, are Top/Center Feed, Side Entry, Conical-Spline, and other intakes. The Top/Center Feed, Side Entry, and Conical-Spline Intake Concepts were evaluated through simulation. Several geometric variations of the three main concepts were also simulated. Each intake was modeled to make as many aspects as comparable as possible. A goal of the paper was to focus on comparing plenum concepts which required separating the effects of runner length and restrictor design from the concepts. The choice of plenum layout directly affects the packaging and design of the runners and restrictor, thus the desire to determine the best suitable intake plenum concept first. With differences in engine, exhaust manifold, intake volume and runner length removed from the simulation, it was possible to determine the most desirable overall geometry that gave the best volumetric efficiency characteristics.

Each intake concept was simulated using industry standard engine simulation software by Ricardo. Ricardo WAVE was first used to model the intake in a full engine model. No changes were made to the base engine model. Each intake concept was then run using a WAVE-VECTIS coupled model. The WAVE simulations modeled the engine across the entire RPM range, while the coupled models are only run at three RPM points due to the much higher computational cost. The coupled model simulated the intake manifold using the Ricardo VECTIS 3D Computational Fluid Dynamics (CFD) code coupled to the rest of engine model simulated by WAVE in 1D. Thus, in the coupled model, the intake manifold is represented in 3D, instead of 1D. Previous researchers have found detailed CFD and coupled 1D/3D methods advantageous in designing intake manifolds. [1-6]

The use of grid convergence analysis tools and best practice methods indicate that reliable coupled solutions were achieved. 1D WAVE only solutions consistently over-predicted 1D/3D WAVE-VECTIS solutions in terms of volumetric efficiency. A steady-state solution was also run that showed a large difference between flow characteristics of the steady state and the WAVE-VECTIS solution. The use of WAVE-VECTIS results to calibrate WAVE resulted in greatly improved agreement between the two simulation techniques. Normal WAVE model calibration would involve the collection of empirical flow data to provide more appropriate representation of the actual pressure losses.

WAVE-VECTIS results offered valuable insights into the internal flow within the intake concepts evaluated. It was possible to locate flow separation by evaluating the surface shear stress as well as by looking at the flow velocity vectors. Likewise, it was possible to see the transport of air-fuel mixture through the intake and air stealing from cylinder to cylinder. In the case of the Top/Center Feed Intake Concept there was very little difference in total pressure loss through 55° packaging bends whether the bend was placed after the restrictor or placed within the runners near the engine.

Results suggest that the Conical-Spline Intake Concept offers the least amount of variation in cylinder to cylinder volumetric efficiency by about an order of magnitude. Because of this, an engine equipped with the Conical-Spline Intake Concept is easier to calibrate and has less acoustic noise content. Using a fuel injection strategy without individual cylinder compensation the Conical-Spline Intake Concept has only a spread of 13.0 to 13.3 trapped Air-to-Fuel Ratio (AFR) from cylinder-to-cylinder. In comparison, the Side Entry Intake Concept has, at its worst, a spread in trapped AFR of 11.5 to 14.0. The Conical-Spline Intake Concept also has diminished half engine order acoustic content and should make muffler design easier as the design can be made to attenuate only a few narrow frequencies rather than a wide frequency range.

The Conical-Spline Intake Concept also resulted in the lowest loss of total pressure through the restrictor. It was observed that the interaction of the restrictor and Conical-Spline Intake Concept often resulted in the choked flow potential of the restrictor's throat being underutilized. In other words, the Conical-Spline Intake Concept at times had the highest volumetric efficiency, but also the lowest percent cycle time of the throat being choked. Even at 14,000 RPM, the throat was choked less then two-thirds of a cycle for all intake concepts. The restrictor ultimately determines peak performance, but at the same time the unsteady nature of the flow results in only partial choked engine operation.

Packaging in the chassis may ultimately decide the intake concept a team chooses. The basic Conical-Spline Intake Concept with straight runners would be very difficult to manufacture for a conventional inline-four cylinder engine. The addition of runner bends to the basic Conical-Spline Intake Concept resulted in greater cylinder-to-cylinder volumetric efficiency imbalance above 10,000 RPM. However, its cylinder-to-cylinder variation performance at high RPM was better than other intake concepts examined.

CONCEPTUAL BACKGROUND

FORMULA SAE INTAKE DESIGNS & CONCEPTS – Initial research focused on understanding and objectively comparing the wide range of naturally aspirated intake manifold geometries exhibited on Formula SAE cars. A simple study was conducted to classify the range of intake manifold geometries used by teams. The study involved the examination of over 100 Formula SAE teams' websites for the latest pictures of a team's intake design. It was found that the field of Formula SAE competitors' intake designs could be classified into three main groups with the rest representing a small percentage of those sampled. Refer to Table 1.

Top/Center Feed Intake Design	Side Entry Intake Design	Conical-Spline Intake Design	Other Intake Design
42%	36%	14%	8%

Table 1. Distribution of Intake Designs

Top/Center Feed Intake Design – This intake is characterized by the placement of the restrictor above and in the center of the row of intake valve ports common to inline four cylinder engines. Thus the main flow axis of the restrictor for this intake layout is symmetric about the two center ports. Some teams use what appears to be an abrupt diffuser entry into the main intake volume. Although, the abrupt diffuser layout had the same classification, it was not modeled. An example of a typical Top/Center Feed Intake design is provided in Figure 1.

Figure 1. Top/Center Feed Intake Design – *University of Texas – Arlington*

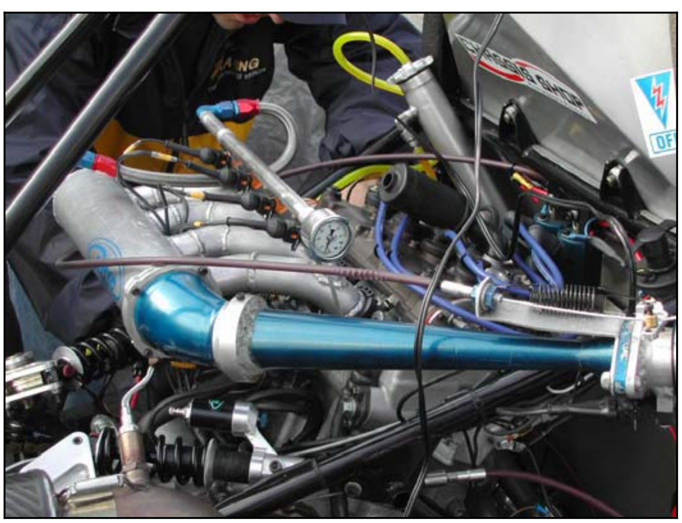

Figure 2. Side Entry Intake Design – *University of Akron*

Side Entry Intake Design – This intake is characterized by the placement of the restrictor to the side of the engine and the main intake plenum volume. The restrictor feeds into the side of the plenum. The main flow axis of the restrictor is not symmetric about any of the ports for this intake layout. Previous researchers have described it as a nonsymmetrical intake. [7] An example is provided in Figure 2.

Conical-Spline Intake Design – This intake is characterized by the placement of the runner inlets in a radial symmetric fashion about the main axis of the plenum. As the restrictor is in line with the plenum, all the runner inlets are symmetric to the main flow axis of the restrictor. The restrictor is typically in the center of the row of intake valve ports common to inline four-cylinder engines. As a consequence of the runner placement and the use of an inline four-cylinder engine, the runners have to be curved to mate to the cylinder head ports. Some of the conical plenums have a true conical shape and are merely an extension of the diffuser angle; whereas others have a spline profile that approaches the conical shape. In this paper the authors refer to a conical intake with a spline profile as a Conical-Spline intake. An example of a conical type intake design is provided in Figure 3.

Figure 3. Conical-Spline Intake Design – *Michigan State University*

Other Intake Designs – For the purpose of this paper the designs that were classified as other, were not investigated. These designs covered a wide range of physical layouts that includes reverse exhaust header styled, variable volume, and dual plenum intakes with each isolated volume feeding two intake ports instead of four. [8]

MAIN MODEL CONCEPT GEOMETRIES USED IN SIMULATION – It was decided to make simplified concept models of the three main designs, with the goal of comparing the merit of each design. The authors considered a design to be an entity that conforms to all engineering specifications, whereas a concept is an entity that doesn't necessarily conform to all engineering specifications. Generally in this paper, designs are physical entities and concepts are merely abstract precursors to detailed designs. After evaluating the concepts, the best one would be selected for detailed design and manufacture. The main goal was to compare the conceptual plenum layouts and keep the runners and restrictor the same. In order to make the concept models comparable some tradeoffs had to be made. The base engine model used throughout this paper was built around a 600cc 4-cylinder Yamaha YZF-R6 engine.

Assumptions Driven By Competition Rules – Wherever possible it was decided to make each concept conform to packaging constraints and the spirit of the rules. To conform to the rules, no intake could protrude outside the envelope of the car defined by the top of the roll hoop and the tires. [9] This rule is in place because of safety concerns with the intake being torn off during a car rollover. Therefore, a side entry intake typically incorporates a bend after the restrictor to comply with this rule, while simultaneously allowing a smooth transition into the plenum. The Top/Center Feed Intake would not necessarily require a bend going into the plenum to meet this packaging rule. However it would require bent runners, a bend going into the plenum, or a bending of the plenum itself. As the primary goal was to compare the plenum layout, the runners were kept the same; and thus the only option was to put a bend in before the plenum. This bend is identical to the bend on the Side Entry intake, which bends through a 55° angle. A 55° bend angle is the approximate minimum angle that complies with the safety rule in our typical in-car installation. Both bends are of a constant and equal diameter.

Assumptions Driven By Need to Keep Intake Concepts Comparable – In the case of a restricted engine, the total volume after the restrictor throat is of prime importance for pressure recovery. In general, an increase in volume after the restrictor throat will tend to increase volumetric efficiency high in the RPM band. To make each intake comparable to one another, the volumes of all plenums were made to be equal within the geometric confines of each model. However, because each intake geometry is slightly different, arbitrary surface boundaries had to be selected to define the plenum volume.

Since all models used the same restrictor, the exit plane of the restrictor diffuser defines the beginning of the plenum volume. Everything after the exit plane of the diffuser and before the entry to the runners is considered plenum volume, for the sake of comparability. Since two intakes have a bend and one does not, the bend must be included in the total plenum volume. The plane that defines the bottom of the plenum (or the start of the runners) defines the other boundary of the plenum volume. The portions of each intake that are defined as plenum volume for each intake concept are shown as a shaded region in Figures 4 through 8.

Each model has an identical restrictor, throttle body section, inlet bell mouth, and air box; the size and design of the intake runners were the same for all three. In all modeled concepts the runner length was held constant at 115 mm. The intake runner spacing and form were designed to be used with a Yamaha R6 engine. The runners are oval in cross section to match the Yamaha R6 ports. This oval cross section runs the entire length of the runner. In addition, the runner has a slight taper. Runner spacing was also modeled identically between the Side Entry and Top/Center Feed intakes.

Figures 4, 5, and 6 show the final CAD representations of the three main intake concepts that were modeled with 1D/3D simulation techniques. Again, the shaded regions depict equivalent plenum volumes.

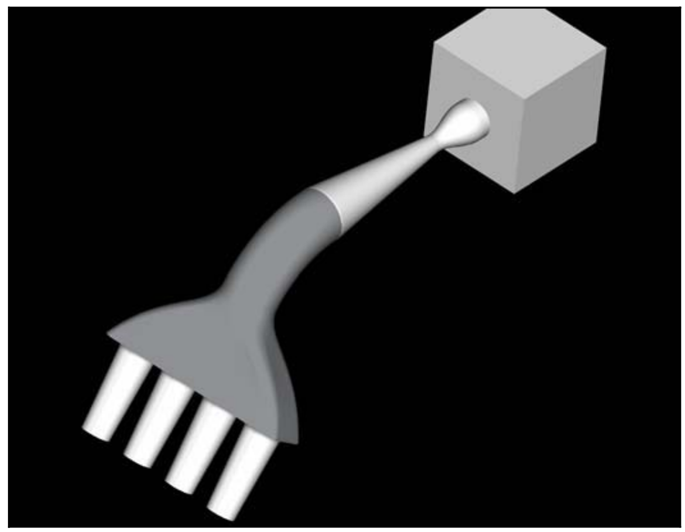

Figure 4. Top/Center Feed Intake Concept

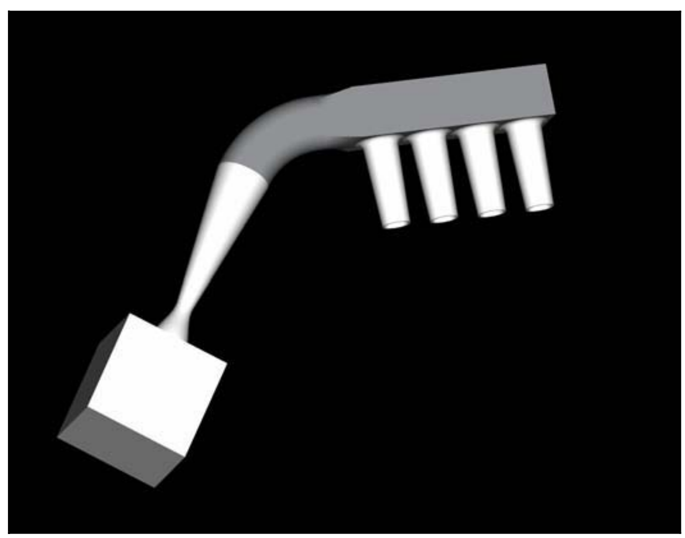

Figure 5. Side Entry Intake Concept

Assumptions Specific to Conical-Spline Intake Concept – Realistic packaging of the Conical-Spline Intake with an inline four-cylinder engine would require longer and curved intake runners. It was decided not to model the longer curved runners in the primary simulation because of the impact these longer runners would have on the torque curve, as illustrated later in this paper. Also, the consideration of different runner lengths would distract the authors from a complete examination of the actual impact different plenum geometries had on performance.

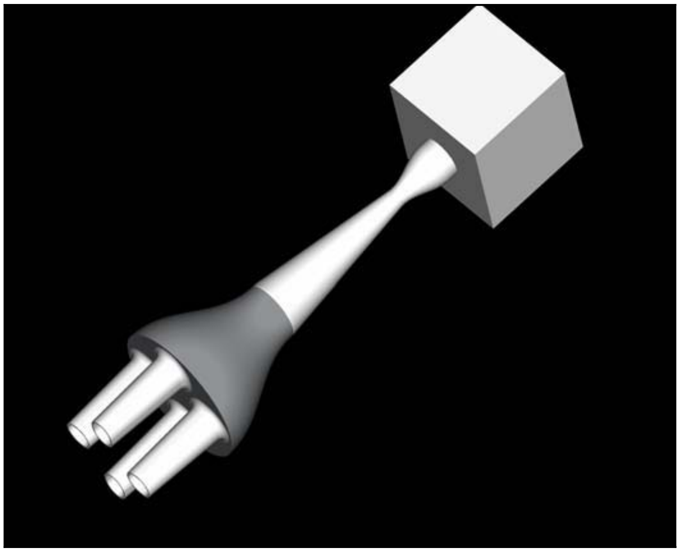

Figure 6. Conical-Spline Intake Concept

With this intake, there is no bend after the restrictor. On an actual engine, the Conical-Spline intake must have bent runners. Thus a bend after the restrictor would not be needed to package the intake as the bending of the runners would serve this purpose. As a sub-concept, a model was created of a Conical-Spline intake system that had bent runners and that would mate to a Yamaha R6 engine.

It was hoped that after an optimum plenum concept is selected that a team would then use the fast turn around time of a 1D simulation code, such as Ricardo WAVE to find optimum runner lengths and volume for the overall intake and exhaust package for its particular engine and design philosophy. Other researchers have developed methods using the quick processing of 1D codes to optimize intake designs. [10, 11] With the Conical-Spline type intake there also exists a real minimum runner length due to the nature of the plenum and runner layout, which must be weighed against any perceived optimum runner length.

SUB-CONCEPT GEOMETRIES USED IN SIMULATION - To ensure that the merit of all the intake concepts were compared fairly, some additional sub-concept plenums were generated. These allowed slight deviations in certain areas while still remaining comparable.

<u>Top/Center Feed Intake Concept With a 55° Bend in the Runners</u> - This concept was run in an effort to evaluate removing the bend between the restrictor and plenum and moving the required bend to the runners. The volume of the bend that was removed was placed in the plenum. The plenum is geometrically similar to the base Top/Center Feed Intake Concept model, with only the total length of the volume changing. As before, the shaded region shows the intake that is considered to be the equivalent volume. Figure 7 shows the Top/Center Feed Intake Concept with the bend in the runners and no bend before the plenum.

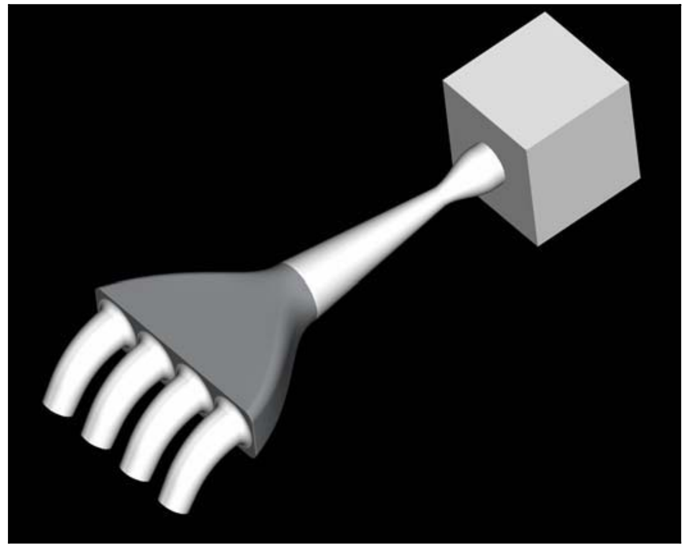

Figure 7. Top/Center Feed – Bent Runners – No Bend Before the Plenum

<u>Conical-Spline Intake Concept With Realistic (Bent) Runners</u> – The authors also evaluated the base Conical-Spline Intake Concept geometry with bent runners as shown in Figure 8. The runners in the Conical-Spline Intake Concept With Bent Runners are curved so that they align with the layout of a Yamaha R6 cylinder head, yet are all of equal length. Thus, the Conical-Spline/Bent Runner intake represents an intake that can be packaged on the car. The main point of interest in running this sub-concept was to determine if the bent runners would have a significant effect on volumetric efficiency in either magnitude or cylinder-to-cylinder distribution.

In Figure 8, cylinders 1 and 4 connect to the outside runners, and cylinders 2 and 3 connect to the inside runners. The runners for cylinder 1 and 4 are a mirror of each other, as are the runners for cylinder 2 and 3. However, the total amount of runner bend (from plenum to port) is different from the inside runners (cylinders 2 and 3) to the outside runners (cylinders 1 and 4). Some teams have packaged runners as shown in Figure 8, but others have had equal curvature runners for all cylinders for a Conical-Spline Intake Concept.

This intake geometry also uses round, constant diameter runners instead of tapered oval runners. The runners also have the same centerline length of 115 mm as used in the Conical-Spline Intake Concept model. It should also be noted that it would be very difficult to package runners any shorter than 130 to 150 mm and still maintain equal length runners, with this intake design. But the design can be tested conceptually against other concepts without concern for detailed analysis of physical packaging limitations.

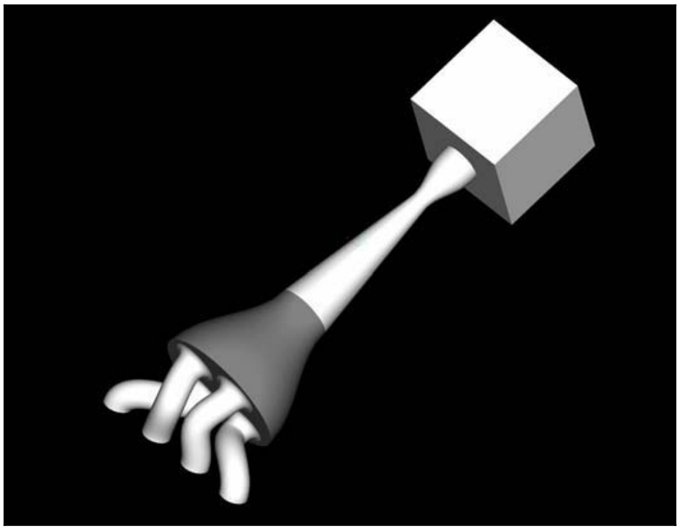

Figure 8. Conical-Spline Intake Concept with Bent Runners

DESCRIPTION OF 1D METHODS

WAVE SOLUTION THEORY – WAVE models engine gas exchange processes within the engine by reducing the intake to a network of 1D ducts and junctions. The WAVE modeling method inherently respects mass, momentum, and energy conservation equations 1 through 3 respectively. [12]

$$\frac{\partial \rho}{\partial t} + \frac{\partial(\rho u)}{\partial x} = 0 \qquad (1)$$

$$\frac{\partial(\rho u)}{\partial t} + \frac{\partial}{\partial x}(\rho u^2 + P) = \frac{\partial}{\partial x}\left(\frac{4}{3}\mu \frac{\partial}{\partial x}\right) \qquad (2)$$

$$\frac{\partial(\rho e_T)}{\partial t} + \frac{\partial}{\partial x}\left(\rho u e_T + P u\right) = \frac{\partial}{\partial x}\left(\frac{4}{3}\mu u \frac{\partial u}{\partial x} + k\frac{\partial T}{\partial x}\right) \qquad (3)$$

The engine model consists of a series of small volumes and a finite difference method is used to solve the mass, energy, and momentum equations. The partial differential equations are solved on a staggered mesh; mass and energy are solved within the discretized volumes and momentum is solved at the boundaries between discretized volumes. Thermodynamic fluid properties are based on the appropriate governing relations. The time-differencing is based on an explicit technique, as the maximum time-step is governed by the Courant condition. [13]

DESCRIPTION OF 3D METHODS

VECTIS THEORY – VECTIS solves a set of conservation equations similar to WAVE. The continuity, energy, momentum, and species transport equations are formulated using a finite-volume approach. The conservation equations are solved implicitly using the following algorithm, Figure 9 with PISO corrector steps. This results in a linear algebraic system of equations for each variable which is solved using a Jacobi/Orthomin with Diagonal Preconditioning method. [14]

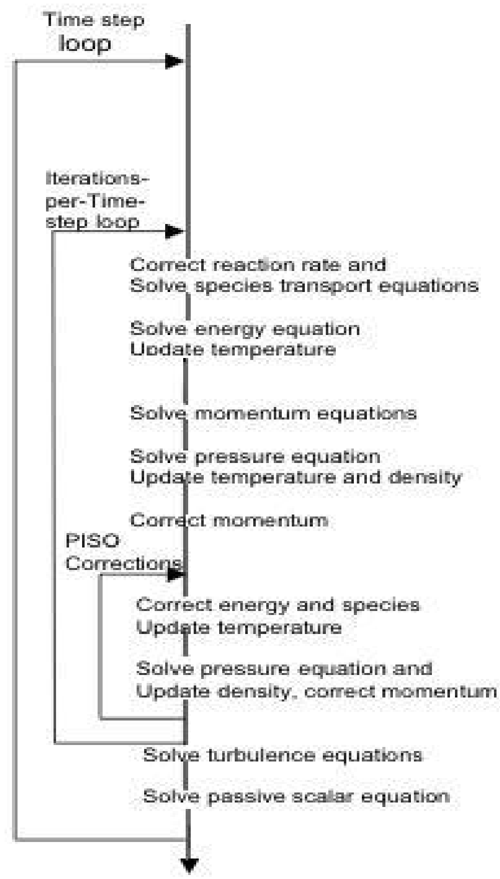

Figure 9. VECTIS Solution Algorithm of Conservation Equation with PISO Corrector Step

Even though VECTIS uses an implicit solver, it was found from experience that the maximum instantaneous Courant number generally could not exceed 1.5. However the authors generally had a target Courant number of 1.0 or less.

Limitation of Steady-State VECTIS Solution – It was found that a full CFD steady state solution of an intake manifold offers little insight into the design when compared against a fully coupled unsteady solution. For comparison, a steady-state solution of the Top/Center Feed Intake Concept was completed. The inlet stagnation pressure was set to 100 kPa and the static pressure at the runner outlet was set to 80 kPa. The static pressure at the runner outlet was based on observation of the typical average static pressure of the unsteady solution at 14,000 RPM. It was found that the unsteady solution contained supersonic flow, but the steady solution with constant pressure drop across all four runners was strictly subsonic. The difference in individual runner mass-flow between the unsteady time-averaged solution and steady-state solution is shown in Table 2. The steady solution predicted that runners 2 and 3 would receive the predominate share of air flow. This prediction is the opposite of what WAVE-VECTIS predicted. However, notice the two predictions give opposite results even though the combined mass flow through all of the runners is within 1.2%, between the steady and unsteady runs. Likewise the qualitative differences between the flow fields for the steady and unsteady time-average solutions were noticeable.

	Average Mass Outflow at Outlet Boundaries [kg/s]				
	Runner 1	Runner 2	Runner 3	Runner 4	Total of All Runners
Time Averaged Unsteady Solution (WAVE-VECTIS)	0.0189	0.0177	0.0177	0.0192	0.0735
Steady State Solution (VECTIS)	0.0165	0.0195	0.0213	0.0153	0.0726
Percent Difference Referenced to Unsteady Solution	-12.7%	10.2%	20.3%	-20.3%	1.2%

Table 2. Comparison of Runner Mass Flow for Unsteady and Steady Solution Methods

Solution Convergence Criteria – Two indicators of convergence for the coupled solution were used. At every time step of the coupled unsteady calculations, the quantities of momentum, pressure, enthalpy, and turbulence were typically solved to a residual error level of 10^{-5} to 10^{-6}. Also, the global indicators of individual cylinder volumetric efficiencies were used as a guide of convergence when changes in solution were less than 0.5%. Figure 10 shows the typical convergence rate of the individual cylinder volumetric efficiency for a WAVE-VECTIS run.

Choice Of Turbulence Model – VECTIS offers two types of turbulence models: standard k-ε and RNG k-ε. It was decided to use the standard k-ε model based on the recommendations of the VECTIS user manual. [14] Even though the k-ε model has known limitations such as dilation effects on turbulence production in highly compressible flow and trouble predicting boundary layer transition and separation, the k-ε model is popularly accepted and used in industrial CFD applications. [15, 16]

The default k-ε model coefficients were used as shown in Table 3. There were insufficient resources to further explore the effects of the turbulence model on the solution accuracy. Other studies have found the effects of different initial turbulent intensities to be slight. [17]

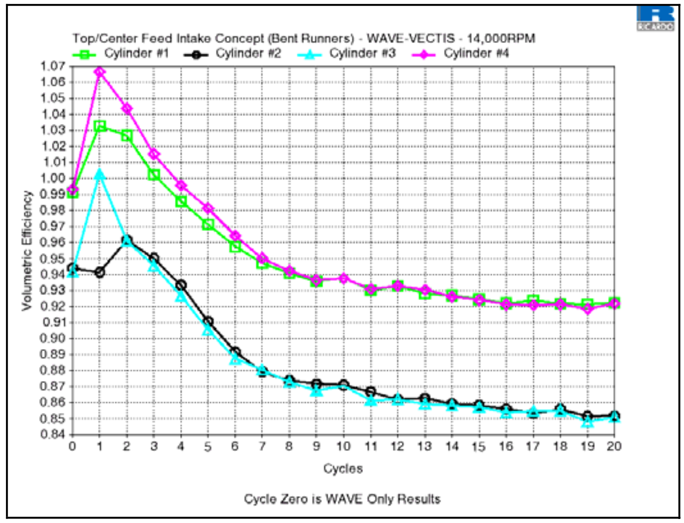

Figure 10. Convergence of Individual Cylinder Volumetric Efficiency for a coupled WAVE-VECTIS Run

C_μ	C_1	C_2	σ_κ	σ_ε
0.09	1.44	1.92	1.0	1.2174

Table 3. k-ε Turbulence Model Coefficients Used in VECTIS CFD Intake Model Simulations

WAVE-VECTIS BOUNDARY CONDITIONS

BOUNDARY CONDITIONS – The boundary conditions in the WAVE model were fixed to 300 K and 100 kPa at the inlet boundary and floating at the exhaust boundary. VECTIS boundary conditions were determined by the WAVE calculation at the inlet and exits for the intake. VECTIS uses a prescribed mass flow forcing at the boundaries as determined by WAVE. The five species present in parts of the flow are air, fuel vapor, burned air, burned fuel, and liquid fuel. Continuity is preserved across WAVE-VECTIS boundaries for all five species. The walls of the concept intakes modeled in VECTIS had a specified temperature of 300 K and a perfectly smooth wall surface roughness.

In an effort to reduce the effect of forcing the boundary conditions on the results of the 3D CFD simulations, all three of the intake concepts included additional features. Each intake had a box with dimensions of 152.4 mm (6.00 in) per side placed near the inlet of the intake where the WAVE and VECTIS codes meet. See Figure 11. In addition, a significant portion of the overall runner length was modeled with VECTIS rather than WAVE. Both these features had the effect of keeping the boundaries far away from the complex 3D flows and providing a uniform 1D flow at the junction between the codes.

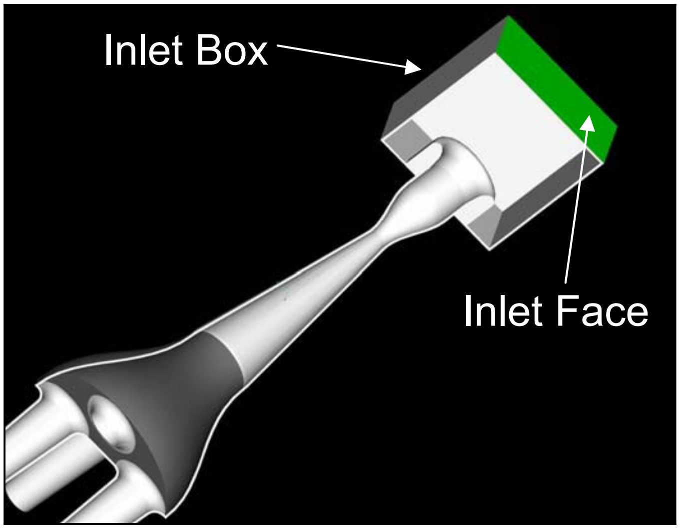

Figure 11. Standard Inlet Box Attached to Every Intake Concept to Move the CFD Boundary Away From the Main Area of Interest

SIMPLIFYING VECTIS INTAKE MODELING FEATURES

FUEL INJECTOR PLACEMENT – Formula SAE intakes typically have the fuel injectors mounted on the intake runners. The VECTIS CFD models for the intakes in this paper included the entire runner length of the intake, up to the cylinder head interface. In order to minimize computational cost and complexity, the fuel injector placement was not modeled with the injector on the intake runner. Having the injector included in the VECTIS model would mean that the fuel spray would have to be included in the 3D CFD calculations, which would increase the complexity of the VECTIS model. Instead, the fuel injectors were placed in a WAVE duct that represents the immediate entry to the cylinder head intake ports. The effect of this is that the fuel injectors are placed within the WAVE model approximately 20 mm downstream from the injector's normal position, which has minimal changes in the model output. In addition, this change eliminated the need to model the injector mounting boss and associated injector hole within the runner portion of the CFD model.

ELIMINATION OF THROTTLE PLATE – In order to reduce mesh size and computation time it was decided to eliminate the modeling of the throttle plate common to conventional throttle bodies upstream of the restrictor. This was considered reasonable as all three intake concepts would still be modeled on equal footing. It has been found by other researchers that complete modeling of the butterfly valve had little effect on overall performance results at Wide Open Throttle (WOT); however this was with a non-restricted engine. [18]

SUPERCOMPUTER USAGE INFORMATION

COMPUTERS USED AND TYPICAL RUNTIME – Simulations were carried out on an IBM SP and an IBM Regatta running multiple processor nodes at the Minnesota Supercomputing Institute. Simulations for the higher RPM data points took around 2500 to 3400 CPU hours on the IBM Regatta. Higher RPM runs required more cycles to converge. The number of CPU hours required depended on the RPM of the simulation and the capabilities of the machine. Models contained up to 750,000 cells, which correlates to a mesh cell size of about 3.5 mm per side and cell size of 1.75 mm per side in the restrictor throat and diffuser area. It was found that the VECTIS code offered fairly linear scalability with an increasing number of processors.

DETERMINATION OF GRID CONVERGENCE INDEX

GCI METHOD BACKGROUND– A goal of this research was to increase the authors' understanding of methods for improving and analyzing the quality of the results of CFD simulation. Due to the financial and technical constraints placed on Formula SAE teams, it is easy to be lead astray by hastily generated CFD results that are at times all too believable and yet at the same time inaccurate. As the CFD community is moving towards improving the quality of CFD results [16], it should be expected that Formula SAE teams should follow that trend.

One method advocated as a standard for reporting the confidence in a CFD solution is the Grid Convergence Index (GCI). [19, 20] The numerical calculation of the GCI begins with at least two solutions of the same problem at two different levels of grid refinement, with both solutions in the asymptotic region of the partial differential equations. Three solutions on three different grids are preferred in that it is rather easy to calculate the observed order of the solution method. From these results, it is a simple matter to assign an error band to the results of the finer grid solution by solving equation 4.

$$GCI[ForFineGrid] = F_s \frac{|E|}{r^p - 1} \tag{4}$$

F_s represents a "factor of safety" applied to the GCI, its value is typically 3.00 when only one level of refinement is used in a grid convergence study and the actual order of accuracy of the simulation is not calculated. F_s can be set as low as 1.25 when two levels of refinement are applied to a problem. With two refinement levels the observed order of accuracy of the numerical method is calculated from the solution and not the intended order of accuracy by the code authors. r is the ratio of the level of grid refinement, and can be thought of as the number of cells in the finer grid divided by the number of cells in the coarser grid. P is the order of the accuracy of the numerical solution method used. E represents the relative error in some particular solution quantity and is found by solving equation 5.

$$E = \frac{f_2 - f_1}{f_1} \times 100\% \tag{5}$$

f represents any possible quantity available in a CFD solution. For example, in a heat transfer problem f could be the global derived quantity of the Nusselt number of a cooling fin, or in an aerodynamics problem the lift coefficient of a wing. The authors chose to look at several solution quantities. The variable f_2 indicates the quantity from the coarser grid and f_1 indicates the quantity from the finer grid. A more detailed description of this and other methods can be found in [20-22].

Calculated Order of Accuracy and Results – Four levels of refinement were tested on the side entry intake concept at 10,000 RPM. Figure 12 illustrates the effect grid refinement had on VE of cylinder number 3. Figure 12 shows mesh tests at global cell sizes of 10 mm, 7 mm, 5 mm, and 5 mm with additional refinement blocks in areas with large flow gradients.

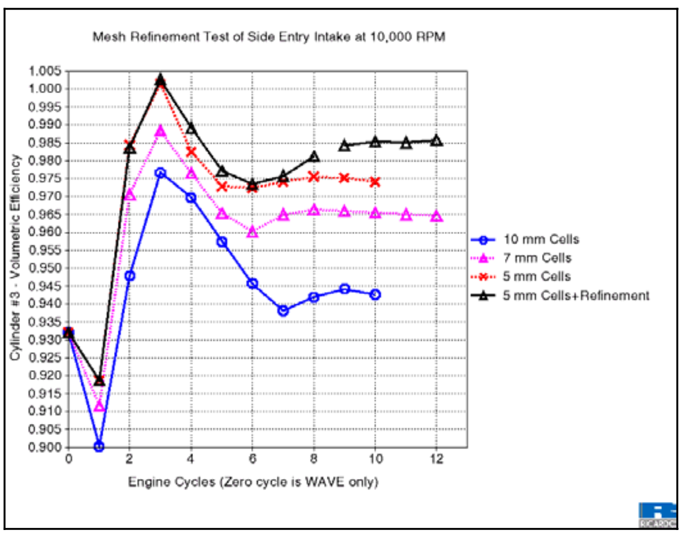

Figure 12. Cylinder #3 Volumetric Efficiency - Solution at Different Grid Refinement Levels

Using the results available from the refinement study similar to what is shown above, and the equation for finding the observed order of accuracy using the three-level grid (Equation 6), it is possible to calculate the observed order of accuracy of the numerical method. It is also possible when using GCI that the observed order and the intended order of the method will not agree due to particular flow phenomena. Shock waves and other discontinuities can alter the effective order of the overall solution produced by a numerical method.

$$p = \frac{\ln\left(\frac{f_3 - f_2}{f_2 - f_1}\right)}{\ln(r)} \tag{6}$$

The effective order of accuracy of the numerical method in the WAVE-VECTIS simulation is approximately 1.5, using the solution quantity of volumetric efficiency for cylinder 3 and treating r as a constant equal to 1.6. The GCI for several engine and flow quantities and are given in Table 4. Many global quantities of interest produced by an engine simulation code coupled to a CFD code are not going to see significant improvements in solution accuracy with increasing mesh refinement. The absolute accuracy of these quantities could be considered loosely coupled to the solution of the CFD grid. For example, the authors made no effort to arrive at an accurate mechanical efficiency number for their engine, so even though the error band around mechanical efficiency could be very tight this should not suggest that the result is necessarily close to reality. On the other hand the authors believe a quantity such as volumetric efficiency is going to be tightly coupled to changes in grid refinement, because this particular quantity is heavily dependent on an accurate solution of intake flow quantities.

In other words, inexperienced users of GCI can get a false sense of confidence in the solution. With a pure fluid dynamics problem, the user's selection of an appropriate turbulence model and application of mesh refinement can result in good GCI or poor accuracy if an inappropriate model is selected. The engine developer is faced with a greater reliance on a multitude of models for such things as friction, combustion, fuel spray transport, and so forth. These models are not going to involve solving complete partial differential equations on the same mesh used to solve the fluid flow problem. As such, good GCI may not always be synonymous with good empirical agreement.

Overall Engine Volumetric Efficiency = ± 0.7%	Cylinder 3 Volumetric Efficiency = ± 3.9%
Absolute Temperature At Monitoring Point Within Diffuser = ± 0.5%	Absolute Pressure At Monitoring Point Within Diffuser = ± 1.1%
Total Time Averaged Mass Flow At Runner #1 Exit = ± 0.7 %	Time-Averaged Total Pressure At Runner #1 Exit Plane = ± 1.6%

Table 4. GCI Expected Error Band for Coupled Simulation Results of Interest

In summary, the process used by the authors for determining the GCI of a given solution quantity begins with three solutions on three equally proportionate sized grids. Then both equations 5 and 6 were solved to provide the necessary values for equation 4 which provides the GCI for the solution quantity.

RESULTS AND EVALUATION OF THE INTAKE CONCEPTS

GENERAL RESULTS – Initially the intake concepts were compared using a WAVE only simulation. The results from WAVE allowed the authors to look at variables across the entire RPM operating band of interest. The volumetric efficiency results for the three main intake concepts (using WAVE only simulations) are shown in Figure 13.

While each intake has the same plenum volume and all concepts were defined to make them as comparable as possible, there are still differences in the VE curves. These differences in VE largely occur between 7,500 to 13,500 RPM, as seen in Figure 13.

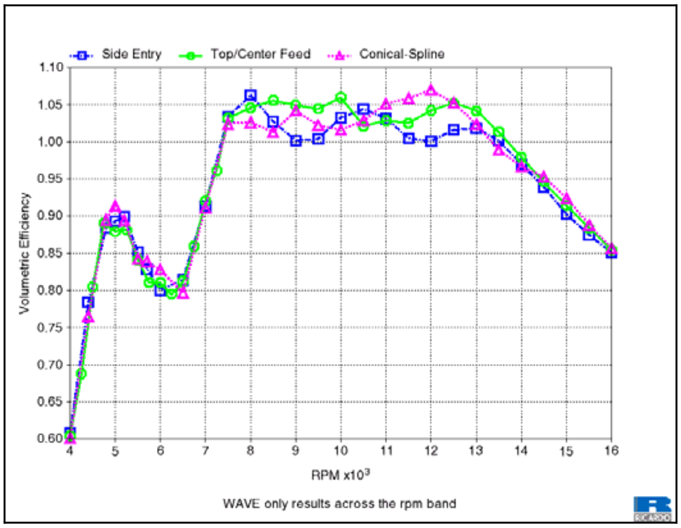

Figure 13. Overall Volumetric Efficiency for the Three Main Intake Concepts (Side Entry, Top/Center Feed With Post Diffuser Bend, Conical-Spline With Straight Runners) from 4,000 to 16,000 RPM

Variations in the Top/Center Feed Intake Concept were investigated. Figure 14 compares a Top/Center Feed Intake Concept with a 55° bend right after the diffuser portion of the restrictor and a similar geometric concept with the 55° bend in the runners. In the latter case the loss of the post diffuser bend volume was made up by an addition of volume to the main volume.

Previous study by the authors found that the distance between the restrictor throat and the runner-plenum junction, offered a limited degree of tuning of the engine's volumetric efficiency curve. This effect probably explains the differences in overall volumetric efficiency as seen in Figure 14.

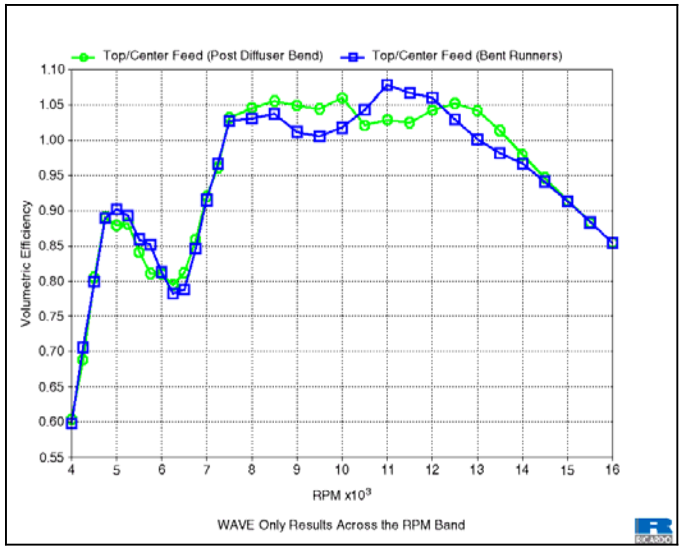

Figure 14. Comparison in Overall Volumetric Efficiency between Top/Center Feed Main Concept and Its Sub Concept

Some intakes such as the Conical-Spline Concept have certain limitations. The Conical-Spline Intake Concept must have bent runners to meet the physical packaging constraints. Due to bent runners, there exists a minimum length that the intake runners must have. This constraint must be considered, and any perceived or real disadvantage must be investigated with respect to one's actual set-up. The authors believe that the runners would likely need to be at a minimum of 130 to 150 mm to be effectively packaged on a typical inline four-cylinder motorcycle engine used in Formula SAE. The minimum practical packaging length is greater than the standard runner length of 115 mm used throughout the simulations. This length represents the distance between the head port and the main plenum volume and not the distance to the valves. However, one should also note that increasing the spacing of the runners at the plenum base would allow the runners to be straighter and thus shorter. Figure 15 shows the effect on overall volumetric efficiency caused by runner length for the Conical-Spline Intake Concept as modeled in WAVE only.

Figure 16 shows the impact bent runners have on the total volumetric efficiency performance of the Conical-Spline Intake Concept with Bent Runners as predicted by WAVE. Notice the VE curve is generally the same but with some loss in tuning effect around 12,000 & 14,500 RPM.

Figures 17 through 21 illustrate the complete WAVE and WAVE-VECTIS individual cylinder volumetric efficiency results for all the intake main concepts and sub concepts. The original WAVE results consistently over-predict in comparison to the WAVE-VECTIS results. There is excellent agreement between WAVE and WAVE-VECTIS results when predicting the cylinder order from highest to lowest volumetric efficiency.

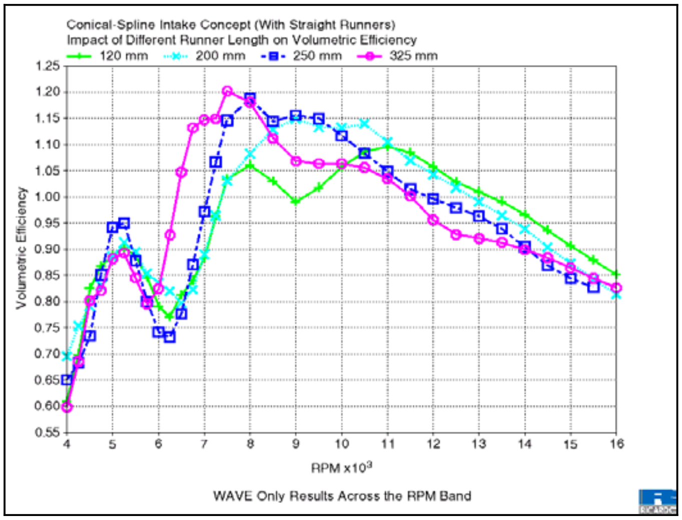

Figure 15. Change in Conical-Spline Overall Volumetric Efficiency Due to Runner Length (125, 200, 250, 325 mm)

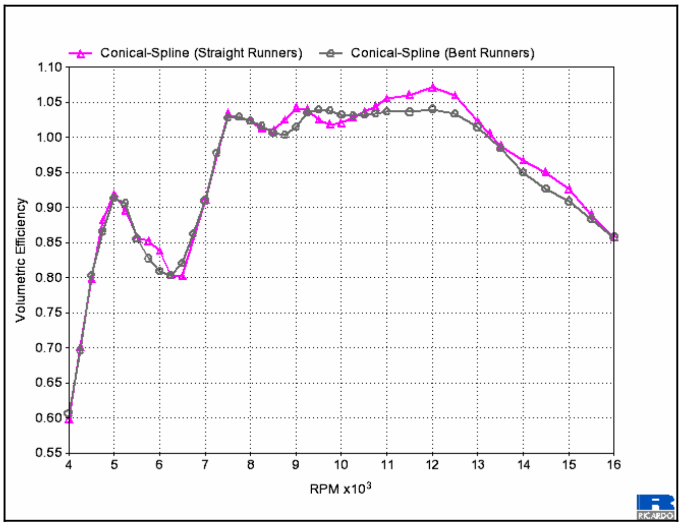

Figure 16. Comparison in Overall Volumetric Efficiency between Conical-Spline Intake Main Concept and Its Sub Concept

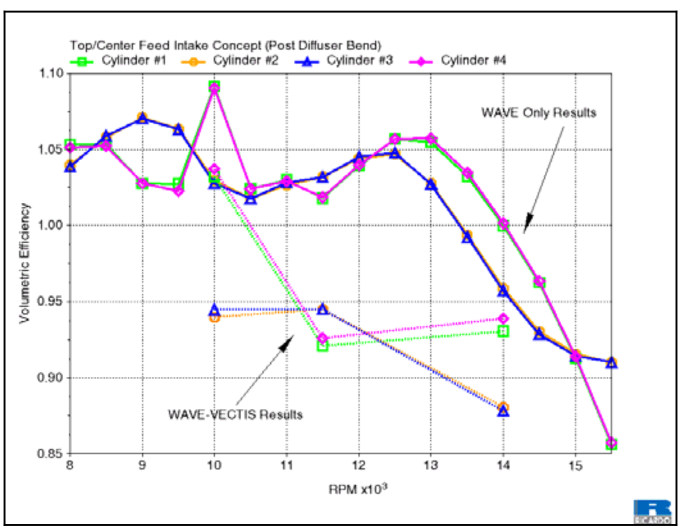

Figure 17. Volumetric Efficiency Results for Top/Center Feed Intake Concept: WAVE Vs. WAVE-VECTIS

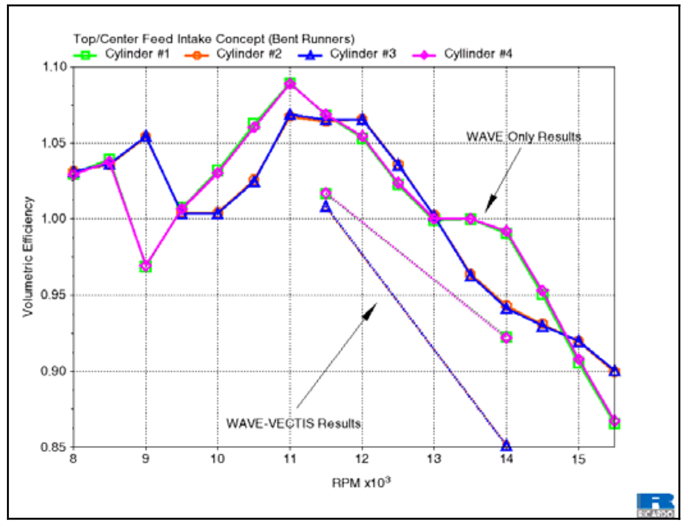

Figure 18. Volumetric Efficiency Results for Top/Center Feed with Bent Runners Intake Sub Concept: WAVE Vs. WAVE-VECTIS

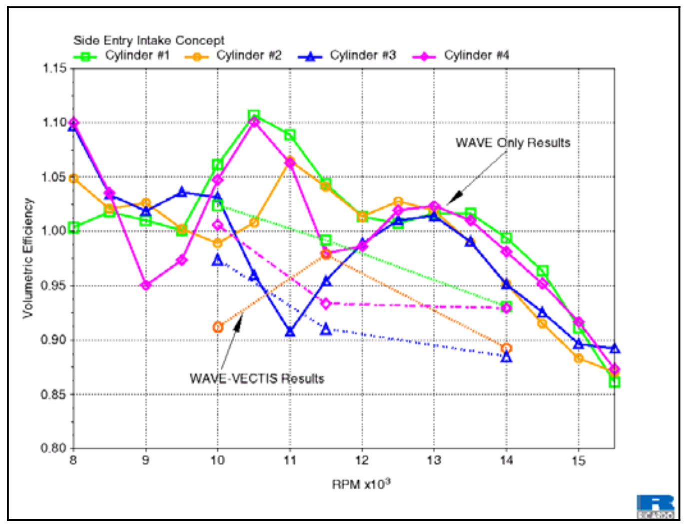

Figure 19. Volumetric Efficiency Results for Side Entry Intake Concept: WAVE Vs. WAVE-VECTIS

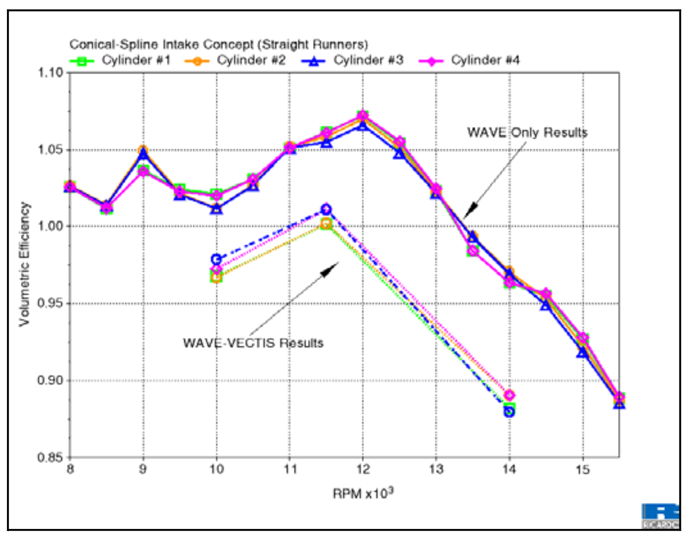

Figure 20. Volumetric Efficiency Results for Conical-Spline Intake Concept: WAVE Vs. WAVE-VECTIS

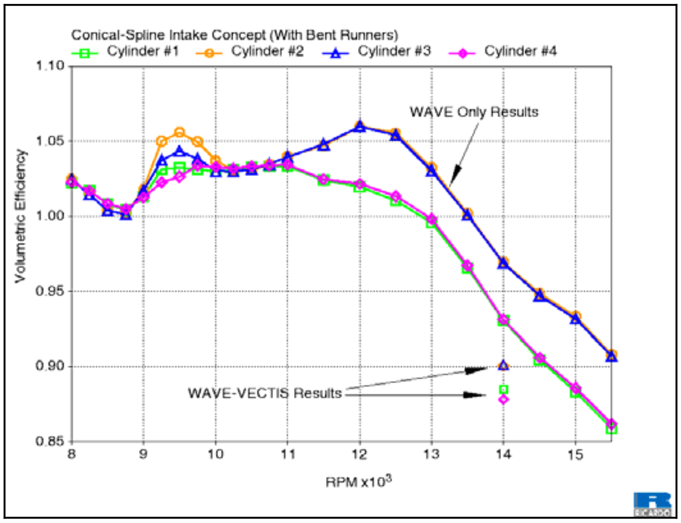

Figure 21. Volumetric Efficiency Results for Conical-Spline with Bent Runners Intake Concept: WAVE Vs. WAVE-VECTIS

The authors believe that a contributing factor in the spread of cylinder-to-cylinder VE is the distance between an individual runner and the restrictor throat and the way this feature impacts tuning. In the case of the Side Entry Intake Concept every cylinder is a different distance from the restrictor throat. For the Top/Center Feed Intake Concept, cylinders and 1 and 4 are the same distance from the restrictor throat and likewise cylinders 2 and 3 are the same distance from the restrictor throat. For both of the Top/Center Feed Intake Concepts, the VE for cylinders 2 and 3 are always grouped together, and likewise for cylinders 1 and 4. In the case of the Conical-Spline Intake Concept, all four cylinders are an equal distance from the restrictor throat.

Also notice that the Conical-Spline with Bent Runners intake concept, there is a grouping of VE between cylinder 1 and 4, and another grouping with cylinder 2 and 3. This is due to cylinders 1 and 4 having a equal amount of total bend curvature. The same is true for cylinders 2 and 3. Also runners 1 and 4 have more total curvature along the bend than runners 2 and 3.

CYLINDER-TO-CYLINDER VOLUMETRIC EFFICIENCY IMBALANCE – A statistical quantity known as the Average Absolute Deviation (AAD) was used to assess the degree of cylinder-to-cylinder volumetric efficiency imbalance (Equation 7). This quantity was found to provide more meaning than the typical standard deviation even though both are conceptually similar quantities. The standard deviation uses a squared difference, which tends to amplify the actual imbalance as opposed to the AAD.

$$AAD = \frac{1}{N} \sum_{i=1}^{N} \left| x_i - \bar{x} \right| \qquad (7)$$

The AAD over the entire operating RPM band is shown in Figure 22 for each intake concept as generated by the WAVE 1D simulation code. In addition, the coupled WAVE-VECTIS results are superimposed on top of the WAVE results at the points of 10,000, 11,500, and 14,000 RPM.

WAVE by itself does a good job of predicting the volumetric efficiency imbalance, as the WAVE-VECTIS results are similar in magnitude. However, WAVE typically under predicts the AAD of volumetric efficiency when compared to WAVE-VECTIS coupled simulations. It is also important to note that WAVE predicts the order of volumetric efficiencies (i.e., from highest to lowest) in the same order as WAVE-VECTIS coupled simulations. This is somewhat surprising, as the authors believed the 1D simulation assumptions would have shown more weakness here. [13] To the contrary, in light of its quick turn around time, WAVE is a very good simulation tool for predicting the magnitude and trends of cylinder-to-cylinder imbalance.

Most interesting is that the Conical-Spline Intake Concept has almost an order of magnitude less cylinder-to-cylinder volumetric efficiency imbalance than the other two concepts. (Note the Conical-Spline Intake Concept graph has a different scale.) The WAVE models alone predict this difference, which is confirmed by the coupled simulation. Given the same volume to work with and additional constraints, it would appear the geometry of the intake does make a large difference in cylinder-to-cylinder volumetric efficiency imbalance.

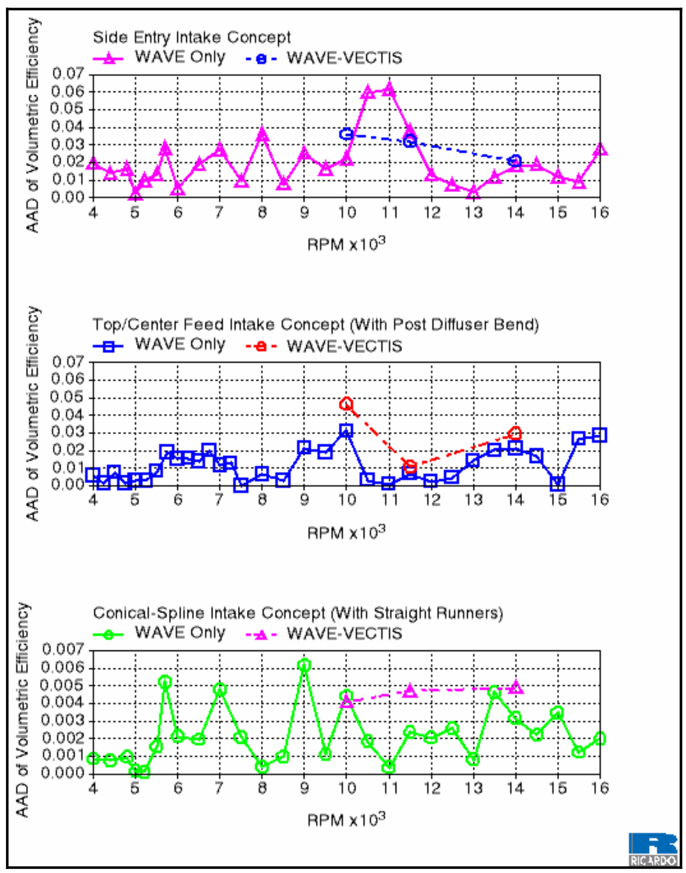

Figure 22. Coupled WAVE-VECTIS and WAVE Only - AAD of VE Results for the Three Main Intake Concepts

Figures 23 and 24 compare the AAD of VE results of the intake sub-concepts to the main intake concepts. Changing the placement of the packaging bend on the Top/Center Feed Intake Concept appears to have little impact on the AAD according to WAVE and WAVE-VECTIS results. Adding bent runners to the Conical-Spline Intake Concept dramatically increases the AAD above 10,000 RPM.

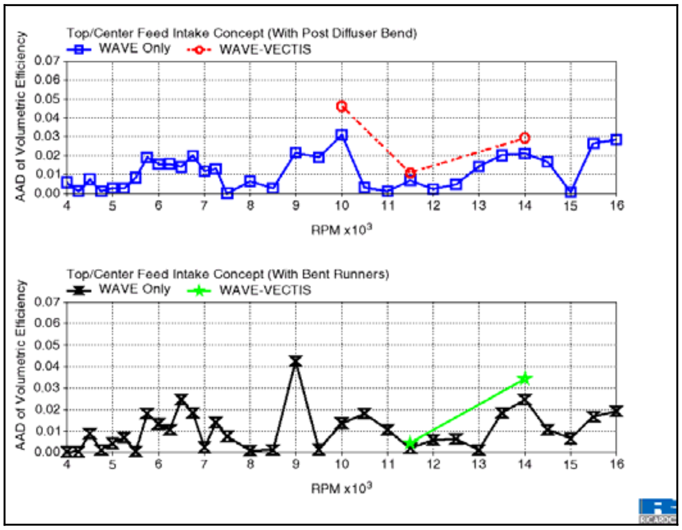

Figure 23. Coupled WAVE-VECTIS and WAVE only AAD of VE Results Comparison between the Top/Center Feed Main Intake Concept and Sub-Concept

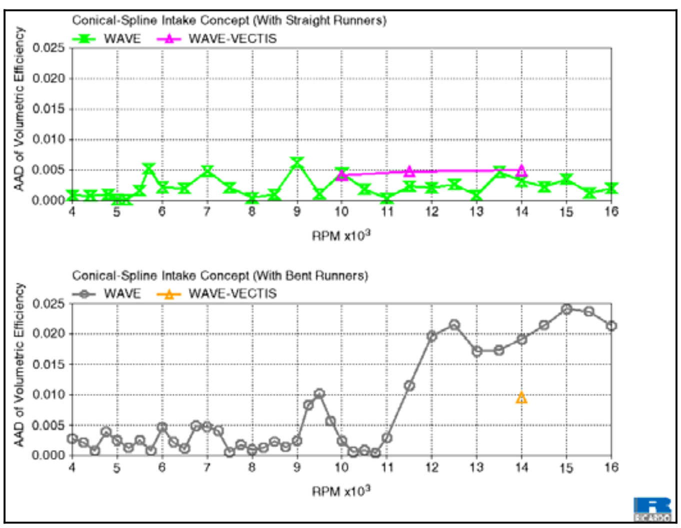

Figure 24. Coupled WAVE-VECTIS and WAVE Only AAD of Volumetric Efficiency Results for Conical-Spline with Straight and Bent Runners Intake Concepts

BENEFITS OF LOW AAD OF VOLUMETRIC EFFICIENCY – Due to lower AAD of VE, the Conical-Spline Intake Concept has additional benefits such as being the most predictable and easiest to calibrate and tune in practice. Also, the Conical-Spline Intake Concept generated a limited range of acoustical frequency content. This may make it easier to pass sound regulations as the designer can target a narrower range of frequencies to attenuate.

Engine Calibration Benefits of Low AAD of Volumetric Efficiency – Minimizing the AAD of volumetric efficiency should help improve performance of the overall engine. A lower AAD of volumetric efficiency means less time spent calibrating fuel and ignition compensations for individual cylinders to achieve maximum performance.

In WAVE, the authors normally set a target AFR that must be met by each cylinder individually. The simulation automatically adjusts the mass of fuel injected for each cylinder individually to maintain the overall target AFR. To examine one effect of the AAD of volumetric efficiency, the authors used an averaged AFR target. The trapped AFR for individual cylinders for each main intake concept is shown in Figure 25. The amount of fuel injected by each injector is held equal, but an overall target AFR controls the amount of fuel injected. Injecting equal amounts of fuel for each cylinder would represent an engine calibration before individual cylinder compensations are introduced. Figure 25 shows that the Conical-Spline Intake Concept offers near equal AFR distribution. Note that the range of AFR on the y-axis of each graph is identical. In the Top/Center Feed Intake Concept, the AFR for cylinders 1 and 4 are grouped together and cylinders 2 and 3 are in another AFR grouping. Referring back to Figures 17, 19, and 20, the AFR grouping matches with cylinder VE grouping. The Side Entry Intake Concept shows the worst control of AFR among the three main intake concepts.

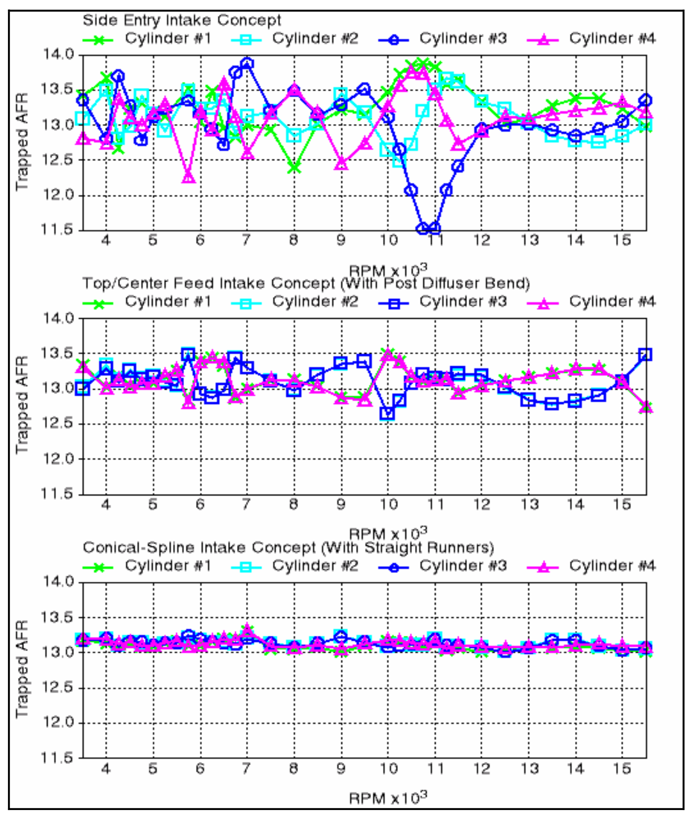

Figure 25. Result of Equal Fuel Injector Calibration on Trapped In-Cylinder AFR for the Main Intake Concepts

Impact of Low AAD of Volumetric Efficiency on Orifice Noise – The rules of the Formula SAE competition require that the complete car does not exceed a certain level of sound emission. Cars are disqualified if they exceed 110 dBA measured at 0.46 m (18”) from the exhaust orifice under static vehicle testing with the car in neutral at a predefined engine RPM. For this particular engine, the sound level measurement is performed at 10,500 RPM.

Both the Conical-Spline and Side Entry intake concepts were run using acoustic quality meshed intakes using WaveBuild3D. WaveBuild3D is a tool used with WAVE to automatically generate complex 1D flow networks from an intuitive CAD representation of the item to be simulated in WAVE. The mesh cell size was set at 15 mm for both intakes. Each model used the same muffler, which also used an acoustic quality mesh. The muffler used prior to the exhaust orifice was a three chamber muffler with packing. The noise level predicted for the engine was performed at 10% load, with the microphone 0.46 meters (18”) away from both the intake and exhaust orifices. WAVE also allows the option of including an empirical flow noise correlation to attempt to model this additional sound source term. However, the flow noise model was not included in these plots.

Figures 26 and 27 show the noise spectrum content for the intake orifices of the Conical-Spline and Side Entry intakes concepts. It should be noted that the plot scales are the same to aid in comparing the two intakes. It is readily apparent that the Conical-Spline shows much less order content than the Side Entry intake. The frequency content shows a wider spread with the Side Entry intake. However, both spectrums do exhibit similar characteristics. It should also be noted that the magnitude of AAD of VE correlates directly with the amount of order content in the sound spectrum. In other words, the Conical-Spline Intake Concept, which had the lowest AAD, also had the least amount of order content.

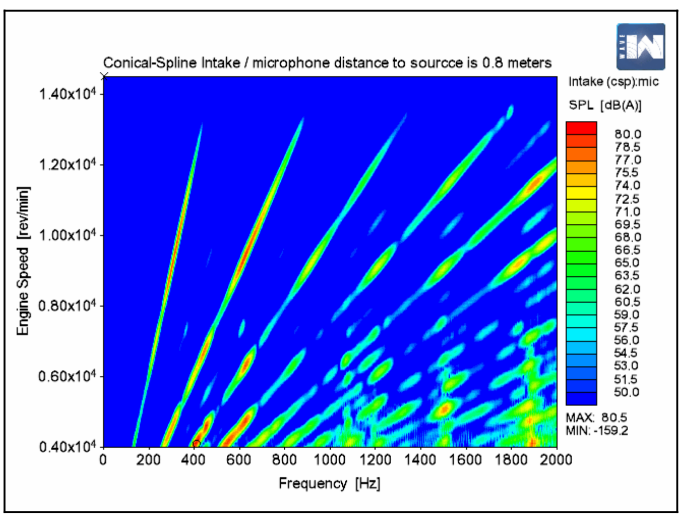

Figure 26. Inlet Orifice Noise from Conical-Spline Intake Concept at 10% Load

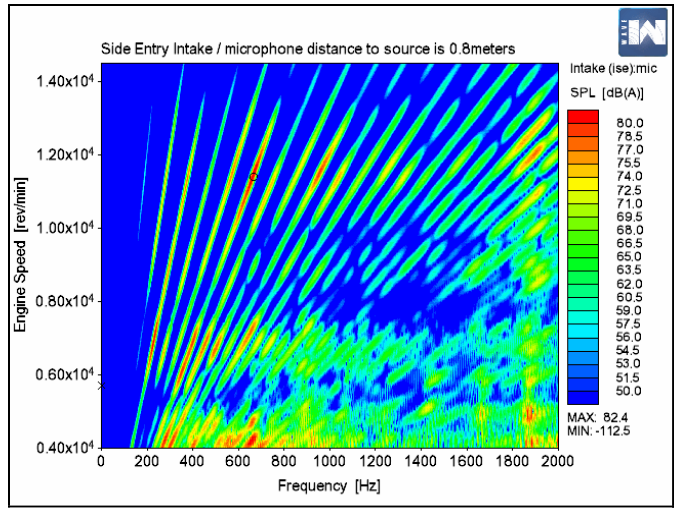

Figure 27. Inlet Orifice Noise from Side Entry Intake Concept at 10% Load

Figures 28 and 29 show the spectrum for the same intake models but of the muffler orifice sound only. It was surprising to observe when only looking at the noise generated at the exhaust tail-pipe that noise spectrum was still impacted by choice the of intake concept. However, the extra order content seen in the Side Entry Intake Concept is at much lower levels than the main order content. The primary content for the exhaust orifice is in 2nd and 4th order for both Figures 28 and 29. Also, the peak spectrum levels from the exhaust orifice are significantly higher than the intake. The same differences in spectrums were also noted when the engine was modeled at wide open throttle.

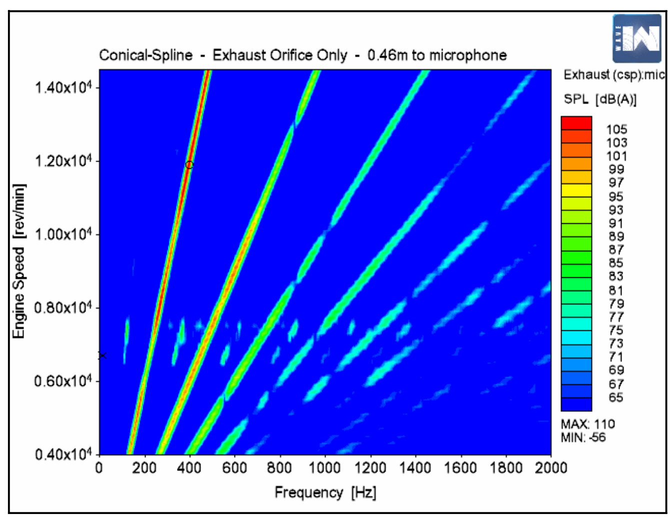

Figure 28. Exhaust Orifice Noise from Conical-Spline Intake Concept at 10% Load

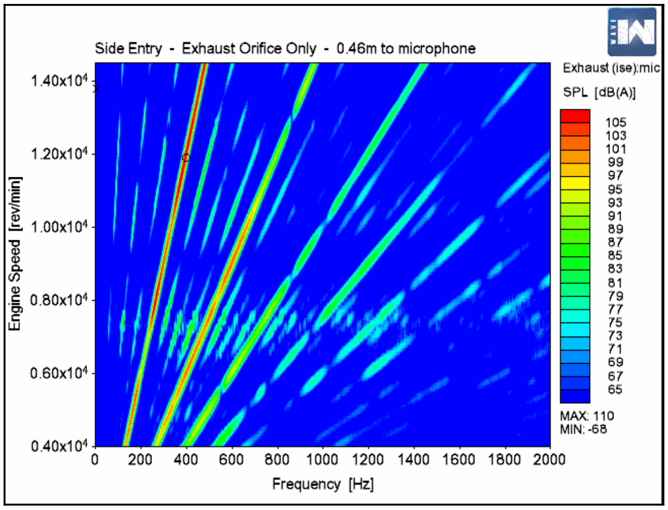

Figure 29. Exhaust Orifice Noise from Side Entry Intake Concept at 10% Load

Figure 30 shows the overall sound pressure level of only the intake orifice noise for the Conical-Spline and Side Entry intake concepts. The Side Entry intake has a higher overall noise level over almost the entire RPM range. Also the Side Entry intake shows its level increasing as the engine speed increases beyond 10,000 RPM, which is the exact opposite effect of the Conical-Spline intake.

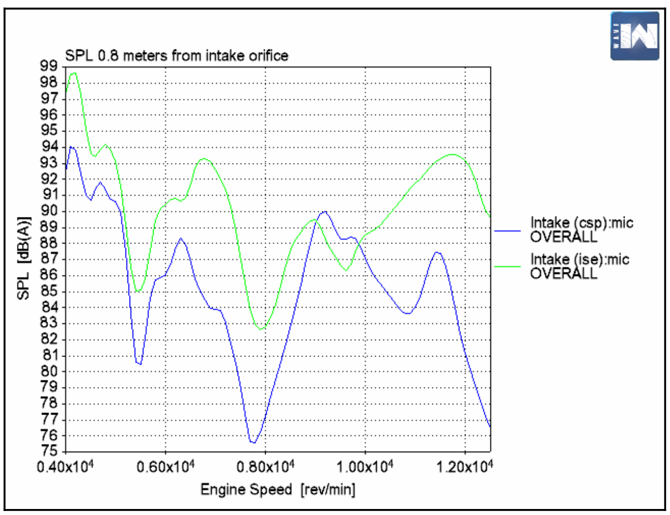

Figure 30. Overall Sound Pressure Level of Intake Orifice Noise for Conical-Spline (blue) and Side Entry (green) Intake Concepts

Figure 31 shows the combined intake and exhaust orifice overall noise level. Both the intake and exhaust orifices are set at a distance of 0.46 m (18") from the test microphone. However, most engine packaging arrangements are unlikely to have the intake and exhaust orifice equidistant from the test microphone. In most typical Formula SAE engine installations the intake orifice is further away from the microphone than the exhaust orifice, and as such the intake noise plays a less important part in the capability of the race car to pass regulations. Thus, Figure 30 likely shows the greatest contribution that the intake might have toward the overall noise level. However, this is only one example, and the contribution of the intake depends, in part, on the effectiveness of the exhaust orifice.

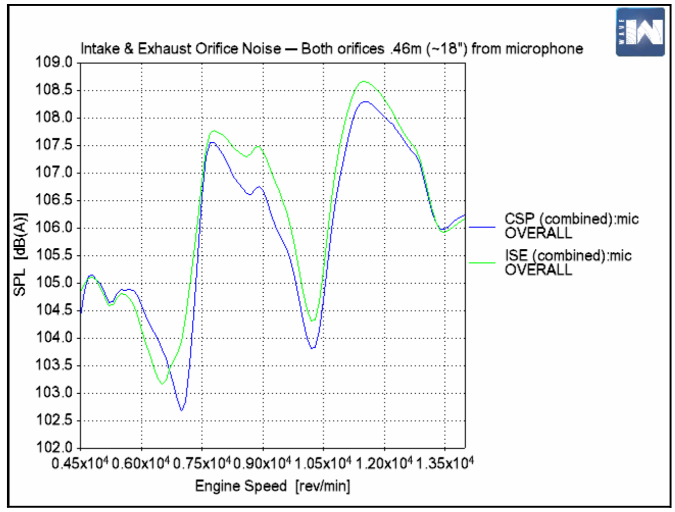

Figure 31. Overall Sound Pressure Level of Combined Intake and Exhaust Orifice Noise for Conical-Spline (blue) and Side Entry (green) Intake Concepts

EFFECT OF PLENUM CONCEPT ON RESTRICTOR FLOW – The authors theorized that the shape of the intake concepts might have an effect on the performance of the restrictor. For example, the main volume of the Conical-Spline Intake Concept at first look appears to be a continuation of the restrictor diffuser and, as such, the authors wished to better quantify any differences between intake concepts.

<u>Mach Number at the Restrictor Throat Over One Engine Cycle</u> – One quantity investigated was the Mach number at the throat of the restrictor over one full engine cycle. This data is also available through the 1D WAVE simulations, but the authors found that the WAVE predictions tended to be very sensitive to the level of discretization. Figure 32 shows a series of WAVE simulations with different levels of discretization along the restrictor and the consequent Mach number predictions. Furthermore, Figure 33 shows the result of a WAVE-VECTIS refinement study at a monitoring point at the center of the throat. The volumes of the finer cells at the throat are 1/8th that of the coarser mesh.

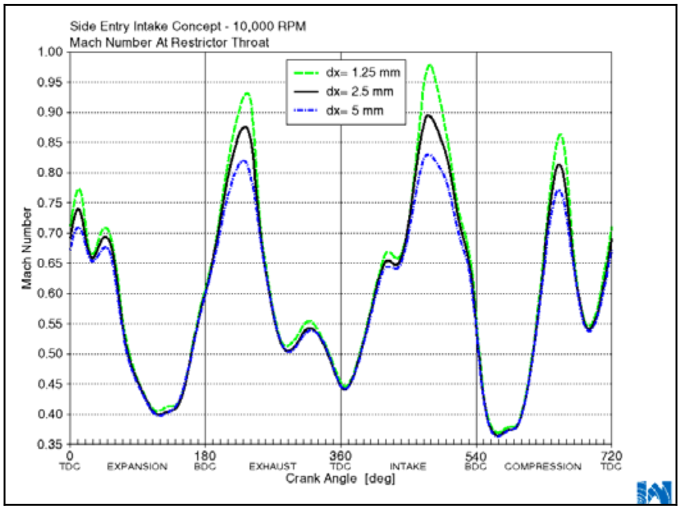

Figure 32. Effect of WAVE Discretization on Mach Number at Throat for Side Entry Intake at 10,000 RPM

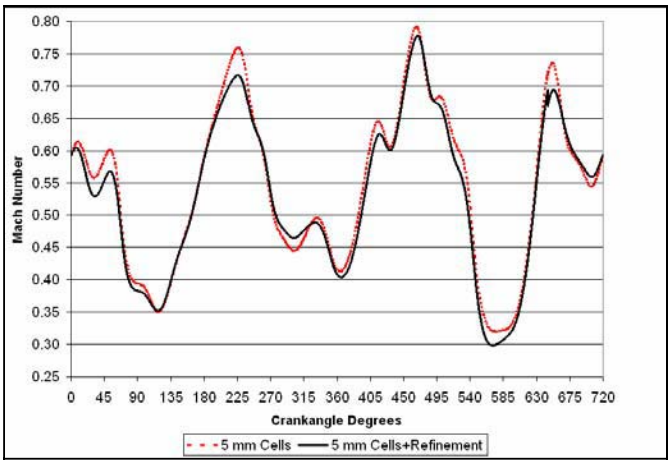

Figure 33. Effect of VECTIS Cell Size on Mach Number at Monitoring Point Near Throat for Side Entry Intake at 10,000 RPM

Tables 5 and 6 provide a summary of the simulation results for the main and sub concept intakes. All results in the tables are based on WAVE-VECTIS simulation results only. It is interesting to observe that even at 14,000 RPM the restrictor throat is not choked all the time. In addition, the amount of time the restrictor is choked does not immediately correlate to which intake has the highest or lowest volumetric efficiency for identical operating conditions.

These observations run counter to the collective wisdom of Formula SAE participants. The results indicate that the restrictor throat is not choked over the whole engine cycle, which is attributable to the unsteady nature of the flow. Similarly, volumetric efficiency is a measure of performance made with respect to the cylinder and not to the throat. As such, the phenomena across the throat have an indirect impact on cylinder filling. The unsteady flow dynamics after the throat and before the intake valves have a direct effect on cylinder filling.

RPM	Main Concept	Time Of Choked Flow %	Total Volumetric Efficiency %	AAD of VE
10,000	Side Entry	0	98.5	0.036
10,000	Top Feed	5.5	98.8	0.046
10,000	Conical-Spline	0	97.2	0.004
11,500	Side Entry	23.6	95.4	0.032
11,500	Top Feed	31.2	93.4	0.011
11,500	Conical-Spline	0	100.5	0.005
14,000	Side Entry	56.9	91.3	0.021
14,000	Top Feed	59.7	90.6	0.029
14,000	Conical-Spline	47.9	87.7	0.005

Table 5. Summary Comparison of Main Concept Intakes Results from WAVE-VECTIS Simulation

RPM	Sub Concept	Time Of Choked Flow %	Total Volumetric Efficiency %	AAD of VE
11,500	Top Feed w/ Bent Runners	34.0	101.2	0.004
14,000	Top Feed w/ Bent Runners	60.4	88.7	0.034
14,000	Conical-Spline w/ Bent Runners	59.0	89.1	0.009

Table 6. Summary Comparison of Sub Concept Intakes Results from WAVE-VECTIS Simulation

Figures 34, 35, and, 36 illustrate the planar time average Mach number of the Conical-Spline and Side Entry intake concepts at different positions along the restrictor. By comparing figures 34 through 36, it is apparent that the physical layout of the intake concept impacts the arrival of pressure pulse at the throat. The odd phasing of pressure pulses arriving at the throat produces an irregular Mach number at the throat. Irregular pressure pulses appear to relate to a greater AAD of volumetric efficiency value signifying greater cylinder-to-cylinder variation.

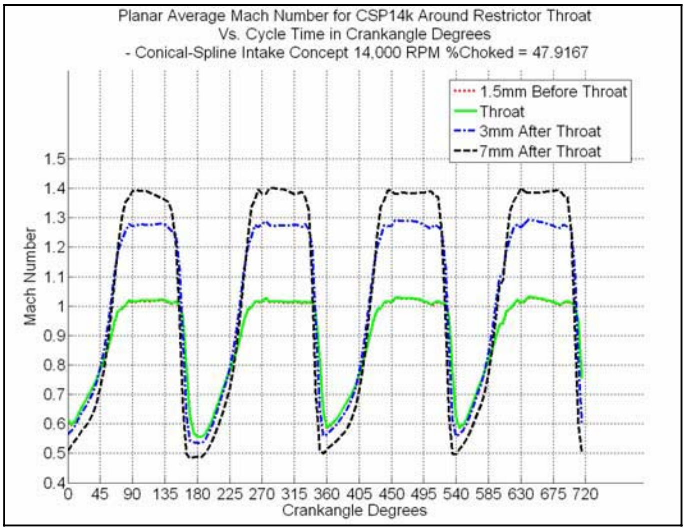

Figure 34. Planar Average Mach Number for Conical-Spline Intake Concept at 14,000 RPM

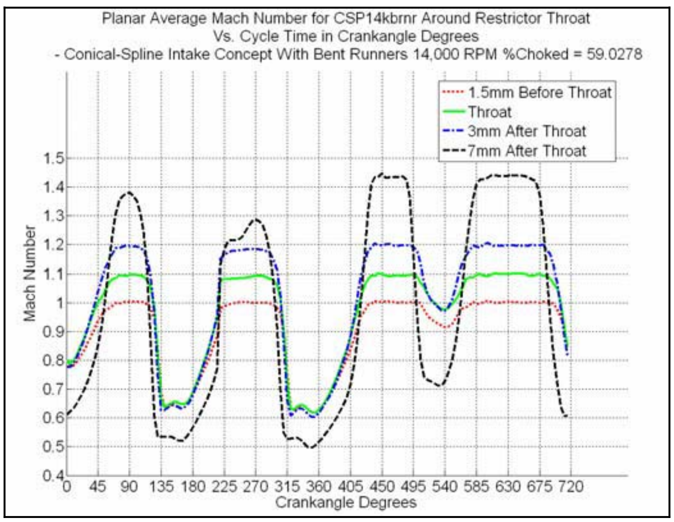

Figure 35. Planar Average Mach Number for Conical-Spline Intake With Bent Runners Sub-Concept at 14,000 RPM

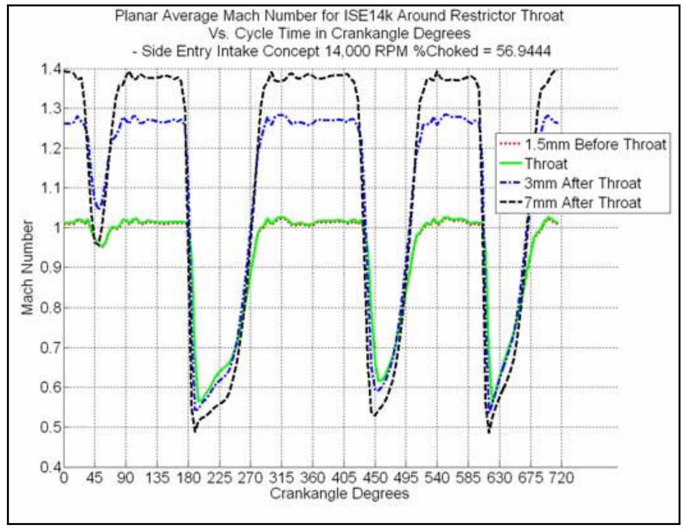

Figure 36. Planar Average Mach Number for Side Entry Intake Concept at 14,000 RPM

<u>Time Averaged Total Pressure Loss Along the Restrictor Diffuser</u> – The authors used the loss of total pressure along the longitudinal axis of the restrictor as a measure of the effect of plenum layout on restrictor performance. Since the simulation is unsteady and includes pressure pulses traveling along the axis of the restrictor's diffuser, a comparison on an unsteady basis could be quite misleading. While the data compared is from unsteady simulation, a time averaged result of total pressure is required to compare one concept to another. This way the effect of pulsed flow on restrictor performance is still captured.

Multiple planes were set up in the VECTIS post-processing software along the main flow axis of the restrictor. The total pressure and distance along the restrictor axis was recorded and analyzed for each plane, using the time averaged result of one engine cycle.

Tables 7 and 8 summarize simulation results for the main and sub concept intakes. Results in Table 7 and 8 are based on WAVE-VECTIS simulation results only. Total pressure drop in the tables was analyzed by looking at the time average solution from a plane at the beginning and a plane at the end of the restrictor that was area averaged. The mean value at each plane was used for the calculation.

The total pressure loss increased with RPM as was expected. As the throat became increasingly choked with increased RPM and as the pressure ratio across the throat increased, supersonic flow in the diffuser arose and consequently there were losses in total pressure due to shocks. In the diffuser, Mach numbers as high as 1.8 were seen at 14,000 RPM.

RPM	Main Concept	Restrictor Total Pressure Drop %	Total Volumetric Efficiency %	AAD of VE
10,000	Side Entry	3.8	98.5	0.036
10,000	Top Feed	6.4	98.8	0.046
10,000	Conical -Spline	3.2	97.2	0.004
11,500	Side Entry	8.8	95.4	0.032
11,500	Top Feed	9.0	93.4	0.011
11,500	Conical -Spline	7.4	100.5	0.005
14,000	Side Entry	18.5	91.3	0.021
14,000	Top Feed	19.0	90.6	0.029
14,000	Conical -Spline	18.2	87.7	0.005

Table 7. Summary Comparison of Main Concept Intakes

RPM	Sub Concept	Restrictor Total Pressure Drop %	Total Volumetric Efficiency %	AAD of VE
11,500	Top Feed w/ Bent Runners	10.1	101.2	0.004
14,000	Top Feed w/ Bent Runners	19.2	88.7	0.034
14,000	Conical-Spline w/ Bent Runners	16.7	89.1	0.009

Table 8. Summary Comparison of Sub Concept Intakes

It was expected there would be an additional total pressure recovery in the case of the Conical-Spline Intake Concept as the main volume of the intake is simply a continuation of the diffuser. In reality, there was negligible change in total pressure beyond the diffuser exit as can be seen in Figure 37. Results for the Top/Center Feed Intake Concept showed similar results, showing negligible changes in total pressure beyond the diffuser.

The Conical-Spline Intake Concept had the lowest loss of total pressure through the restrictor. Whether this is attributable to it also having the lowest AAD of volumetric efficiency is not clear. The Side Entry Intake Concept also exhibits good pressure recovery performance in comparison to the Top/Center Feed Intake Concept, but the Side Entry Intake Concept has the poorest AAD of VE performance.

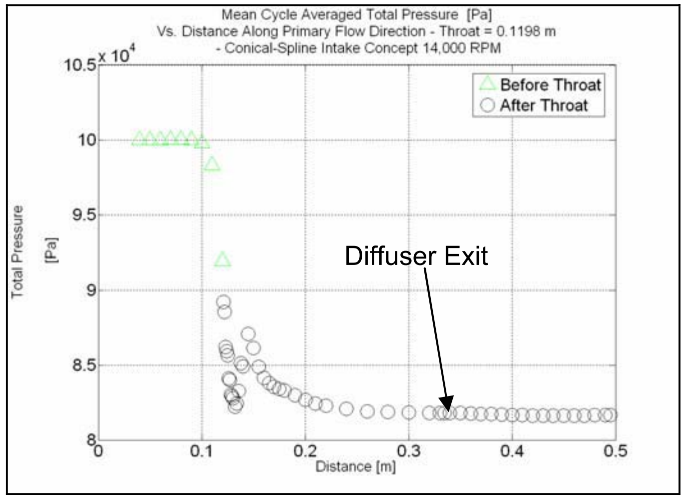

Figure 37. Time Average Total Pressure Along Restrictor for Conical-Spline Intake Concept at 14,000 RPM

ADDITIONAL INSIGHTS OFFERED FROM COUPLED ANALYSIS – A significant benefit offered by the coupled simulation method is the fully 3D flow solution. Nowhere is this more helpful than in visualizing the flow. For example, the authors were startled to see in a plane cut through the Side Entry Intake Concept, a large standing vortex above the intake runner for cylinder 4. This vortex existed over much of the engine cycle at 11,500 RPM and is believed to stem from the nonuniform flow exiting the bend and asymmetric layout of the Side Entry Intake Concept. When the data was time averaged, the vortex was still apparent. The view shown below in Figure 38 is the total velocity vector plane above the runners and the plane is perpendicular to the longitudinal axis of the runners.

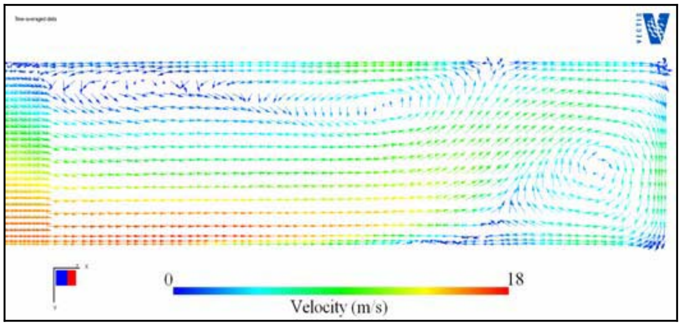

Figure 38. Total Velocity Vector Plot Time Averaged over a Cycle for the Main Side Entry Intake Concept at 11,500 RPM. (0 to 18 m/s)

By looking at instantaneous snap shots of the flow it is also possible to see air stealing between the cylinders. Figure 39 illustrates this phenomena within the Side Entry Intake Concept.

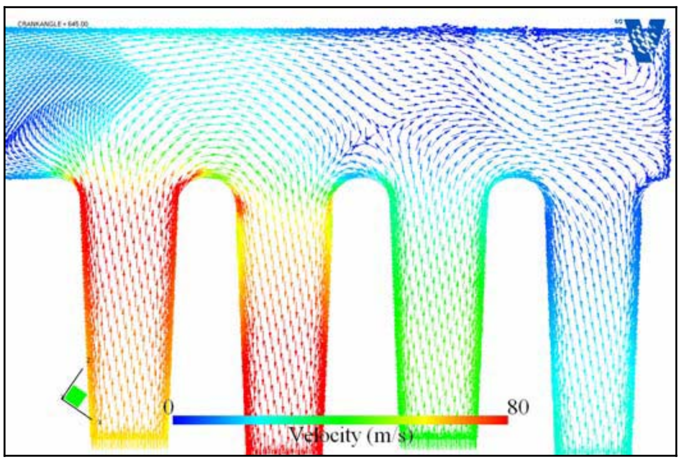

Figure 39. Side Entry Intake at 14,000 RPM Velocity Vector Plot CAD = 645° (0 to 80 m/s)

The visual insight possible with CFD is extremely helpful in this case. Looking at Figure 39, it would be quick work to reason that placing fuel injectors in parallel and aligned with the longitudinal axis of the runners at the top or roof of the intake would make the equitable distribution of fuel very difficult. This is something the authors learned originally from past dynamometer experience and with physical intake prototypes similar to the main Side Entry Intake Concept shown above. The physical explanation would appear to be that the flow is anything but predictable and orderly above the runners.

Since the fuel injectors in the simulation were placed in what would physically be the cylinder ports of the engine and not in the VECTIS model, fuel control in the unsteady flow was excellent. Figure 40 shows the chemical content of the gas inside a portion of the Side Entry Intake Concept. It shows that only a small length of the runner contains fuel and other combustion products, suggesting that engine calibration with the fuel injector as close as possible to the intake port should be predictable.

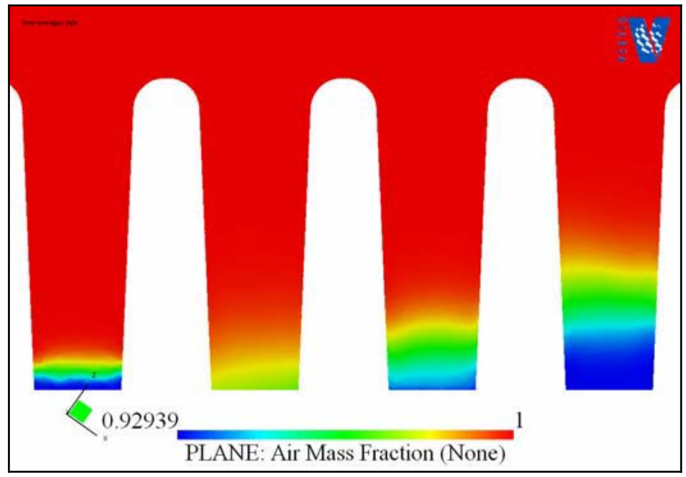

Figure 40. Time Averaged Air Mass Fraction in Side Entry Intake at 14,000 RPM (0.92939 to 1)

<u>Locating Separated Flow</u> – Flow separation generates losses within the intake and as separation is an inherently three-dimensional phenomenon, VECTIS is an excellent tool for identifying these losses.

One symptom of the existence of separated flow is a local drop in surface shear stress. Although observation of surface shear stress is not without limitations [23], the ease of measuring it with CFD makes it a quick indictor of potential losses.

Figures 41 and 42 illustrate the surface shear stress in the Side Entry Intake Concept. Shear stress is high near the throat and beginning portion of the diffuser because the flow velocities are very high. Further down in the diffuser where there are known regions of asymmetric transitory stall and flow separation, the surface shear stress drops in certain areas to near zero. Along the bend, the flow tends to adhere to the inside of the bend and consequently the surface shear stress is higher there.

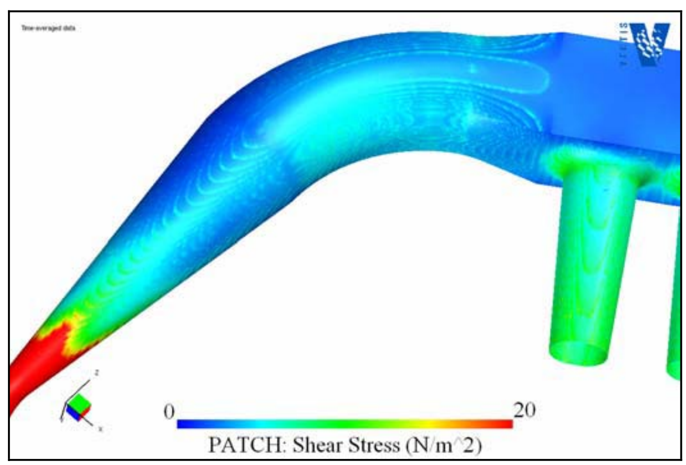

Figure 41. Time-Averaged Surface Shear Stress for Side Entry Intake Concept at 11,500 RPM (0 to 20 N/m^2)

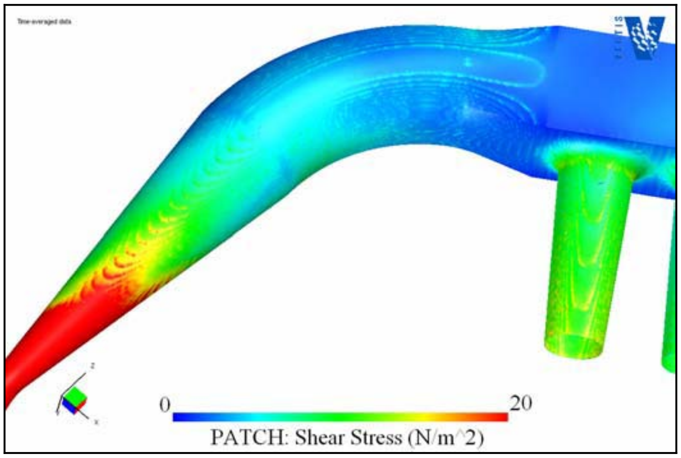

Figure 42. Time-Averaged Surface Shear Stress for Side Entry Intake Concept at 14,000 RPM (0 to 20 N/m^2)

Another way to locate regions of flow separation and pressure loss that is only available in unsteady CFD engine simulation is to look for times where unfavorable pressure gradients and the arrival of pressure pulses can cause the flow to separate. In figures 43 and 44, the velocity vectors in the diffuser are shown for the Conical-Spline with Bent Runner Intake sub-concept at two different portions of the engine cycle.

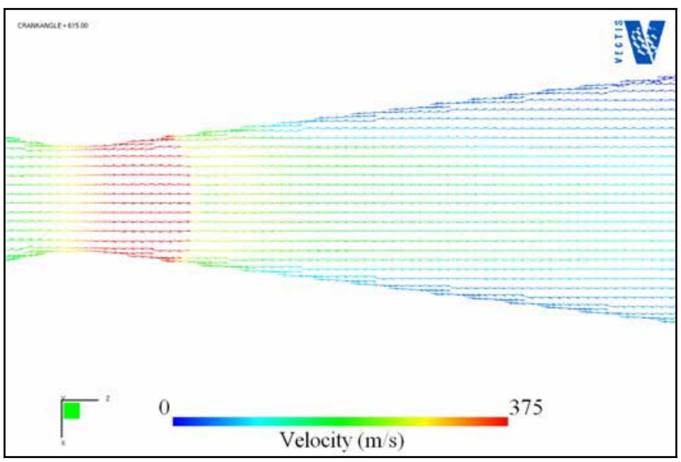

Figure 43. Conical-Spline with Bent Runners Intake Sub Concept at 14,000 RPM Showing Attached Diffuser Flow at 615 Crankangle degrees

Figure 44 illustrates the transient separation caused by the arrival of an adverse pressure pulse in the diffuser. This type of phenomenon cannot be captured with steady-state simulations.

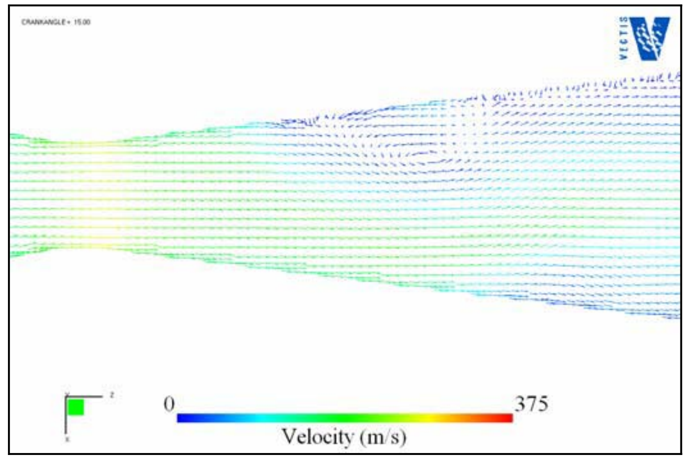

Figure 44. Conical-Spline with Bent Runners Intake Sub Concept at 14,000 RPM Showing Separated Diffuser Flow at 15 Crankangle degrees

Bend Placement for Packaging – Due to the need to keep any intake design within an envelope around the car to comply with Formula SAE safety regulations, some of the intake concepts incorporated bends to improve packaging. In the case of the Top/Center Feed Intake Concept, two reasonable options to aid packaging were identified as either a bend between the diffuser and the main plenum volume or bent intake runners. Table 9 describes the bend geometry model used to investigate the two packaging options. Both options allowed the intake concept to comply with the Formula SAE packaging envelope.

Bend Geometry For Top/Center Feed Concepts		
Feature	Post Diffuser Bend	Bent Runners
Bend Radius	0.1524 m	0.1016 m
Average Cross Section Diameter	0.0727 m	0.0420 m
Bend Angle	55°	55°

Table 9. Description of Bend Geometry Used to Package Intake Concepts per Formula SAE Regulations

The two options were evaluated by determining the total loss coefficient. [24, 25] For the post diffuser bend the loss coefficient K_c, was found by solving equation 8.

$$K_c = \frac{P_{t_1} - P_{t_2}}{P_{t_1} - P_1} = \frac{1 - P_{t_2}/P_{t_1}}{1 - P_1/P_{t_1}} \qquad (8)$$

P_{t_1} and P_{t_2} are equal to the total pressure at the upstream and downstream demarcation, respectively. Similarly, P_1 and P_2 are equal to the absolute pressure at the upstream and downstream demarcation, respectively. The mean pressure values are extracted from planes located at the beginning and end of the bend geometry. In the case of the bent runners where the cross section of the runner decreases slightly along the length of the runner, equation 8 is modified in reference to the downstream conditions as shown in equation 9.

$$K_c = \frac{P_{t_1} - P_{t_2}}{P_{t_2} - P_2} = \frac{P_{t_1}/P_{t_2} - 1}{1 - P_2/P_{t_2}} \quad (9)$$

Table 10 illustrates the results of the total loss coefficient analysis, which are inconclusive. This is believed to be attributable to the limitations of the area averaging method used in VECTIS when it comes to non-uniform flow [26, 27] as well as the unsteady flow solution. It may be preferable to use a steady state analysis to discern which bend layout is more desirable as there have been net reductions of pressure losses in the intake with positive benefits to performance as found by other researchers. [3, 28-30] At this point, the authors favor the use of bent runners to meet the packaging constraints, as the runner bend allows good fuel spray targeting, assuming the runner lengths are reasonable.

Total Loss Coefficients, K_c		
RPM	Top/Center Feed	Top Center Feed w/ Bent Runners
11,500	-0.14	-0.32
14,000	-0.59	-0.49

Table 10. Calculated Total Loss Coefficients Along the Bends Required for Packaging Top/Center Feed Style Intake Concepts

Using Coupled WAVE-VECTIS Results to Tune WAVE – Because of the time invested in performing WAVE-VECTIS simulations, it was important to utilize everything learned from each run. One way of doing this is to use measurements taken from the WAVE-VECTIS results to tune the WAVE only results. Since the areas of interest to the authors are heavily dominated by the flow characteristics within the intake, one way to tune the results was to apply pressure loss coefficients derived from WAVE-VECTIS results to the WAVE model. This technique allowed the accuracy of the WAVE results to improve without the expense of additional computational time.

Figure 45 illustrates the basic result of tuning a WAVE only model. Constant pressure loss coefficients were set with respect to RPM for the Top/Center Feed Intake Concept resulting in better agreement between simulation methods. In reality, pressure losses would be a function of RPM as losses from friction, separation, and shocks are also functions of RPM. It is possible to construct pressure loss coefficient maps to further tune the WAVE results.

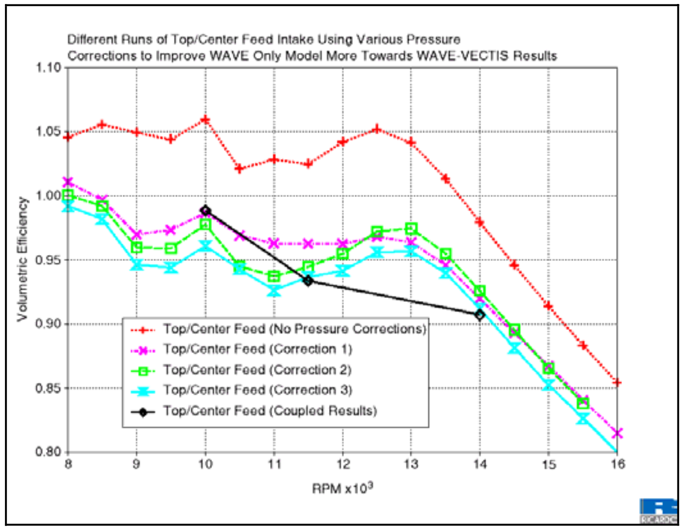

Figure 45. Use of WAVE-VECTIS Results to Tune WAVE Only Results for Top/Center Feed Intake Concept

CONCLUSION

Formula SAE participants field a large variety of intake designs at competition. An analysis of teams' naturally aspirated intake designs showed that 42% of the teams competed with a design classified as Top/Center Feed, 36% competed with Side Entry intakes, and 14% competed with Conical-Spline intakes. The remaining 8% were difficult to classify. The range of intake designs suggests to the authors that Formula SAE participants as a whole have not found the most competitive intake design.

From this analysis, the three most common designs were developed into conceptual models for ease of analysis and comparison using CAD. In order to address packaging constraints resulting from Formula SAE competition rules in the three main concepts, two additional sub-concepts were simulated. These sub-concepts involved changes in bend placement or the addition of more realistic runners for packaging with an inline four-cylinder engine. As a whole, every concept simulated had identical restrictors and total plenum volume. Likewise the runners for the three main concepts all had the same length, diameter, cross section, and taper. The sub-concepts had slightly different runners with the inclusion of a bend.

To assist in evaluating the performance of each intake concept, the AAD of VE was used to measure cylinder-to-cylinder imbalance. The Conical-Spline Intake Concept had the least VE imbalance and the Side Entry Intake Concept had the greatest VE imbalance. AAD of

VE also impacted acoustic order content as well as trapped AFR for an engine calibration strategy that does not involve individual cylinder compensations. A lower AAD of VE correlated well with a reduction in pressure drop along the restrictor.

Going from straight runners to highly bent runners with the Conical-Spline Intake Concept showed an increase in AAD of volumetric efficiency at high engine speeds. With the bent runners, the AAD of volumetric efficiency did not increase significantly until 10,000 RPM. The AAD of volumetric efficiency for the Conical-Spline Intake Concept with Bent Runners was at the same levels as the Side Entry Intake and Top/Center Feed Intakes in the high RPM range. AAD of volumetric efficiency was still very low for the Conical-Spline Intake Concept With Bent Runners at low engine speeds (below 10,000 RPM).

The coupled 1D/3D methods showed that choked flow did not occur during 100% of the cycle, even at high RPM. The Conical-Spline Intake Concept underutilized the choked flow potential of the restrictor as it was generally the least choked on a time basis of all the intakes evaluated for a given RPM. Additional total pressure recovery by smooth continuation of the diffuser into the plenum volume in the case of Conical-Spline Intake concept proved to be negligible.

Using 1D/3D methods provided additional benefits and insights. The detail provided by the 3D methods made finding adverse flow conditions very easy. Diffuser stall and separation were identified as well as air stealing between cylinders. It was also possible to assess the impact of different packaging bend locations needed to conform to Formula SAE rules.

In the Top/Center Feed Intake Concept, placing the bend in the plenum section or in the runners did not largely impact flow losses relative to one another. However, changing the placement of the bend and the allocation of plenum volume did change the intake tuning. The authors believe that between the two Top/Center Feed Intake concepts, the use of bent runners is a better option as it allows better fuel injector targeting and overall packaging.

Concept Selection

The Conical-Spline Intake Concept was chosen as the best overall design. The Conical-Spline Intake Concept offers an order of magnitude reduction in AAD of VE across the RPM range compared to other models. Even with highly bent runners, the Conical-Spline Intake Concept provides lower or equal AAD of VE compared to the other intake concepts. The improved acoustic content and trapped AFR performance of the Conical-Spline Intake should make muffler design and Engine Control Unit (ECU) calibration easier. The Conical-Spline Intake Concept also consistently showed the best pressure recovery along the restrictor of all the intake concepts and sub-concepts.

ACKNOWLEDGMENTS

Special thanks go to our original team advisor Dr. Patrick Starr for initially sponsoring the research work and to Dr. David Kittleson and Dr. William Durfee for continuing their support and sponsorship of our research. The authors would also like to acknowledge the continual assistance of Dr. Birali Runesha and the rest of the support staff at the Minnesota Supercomputing Institute for their help in high performance computing. We would like to thank Ricardo Software and in particular Karl John, Patrick Niven, and Enrico Bradamante for their generous support and advice. We would also like to thank Kim Lyon of Daimler-Chrysler for his expertise and advice regarding engine modeling and calibration. Additional thanks goes to Dr. Bruce Jones of Mankato State University for allowing us to use his department’s flow bench. We would like to thank team members John Kess and Aaron Reinhart for helping us make test fixtures and gather data for the team’s WAVE models.

REFERENCES

1. Pogorevc, P. and Kegl, B., “Intake System Design Procedures for Engines with Special Requirements”, Proceedings of the Institution of Mechanical Engineers, Part D: Journal of Automobile Engineering. Vol. 220, 2/2006, pp 241-252.
2. Maynes, B. D. J., Kee, R. J., Kenny, R. G., Fleck, R., Mackey, D. O., Foley, L., “Prediction of Formula 1 Engine and Airbox Performance using Coupled Virtual 4-Stroke and CFD Simulations”, SAE Paper 2002-01- 3318.
3. Riegler, U. G., and Bargende, M., “Direct Coupled 1D/3D-CFD-Computation (GT-Power/Star-CD) of the Flow in the Switch-Over Intake System of an 8-Cylinder SI Engine with External Exhaust Gas Recirculation”, SAE Paper 2002-01-0901.
4. Strauss, S. T., and Schindler, P., “Code Coupling, a New Approach to Enhance CFD Analysis of Engines”, SAE Paper 2000-01-0660.
5. Borghi, M., Mattarelli, E. and Montrosi, L., “Integration of 3D-CFD and Engine Cycle Simulation: Application to An Intake Plenum”, SAE Paper 2001-01-2512.
6. Laimböck, F. J., Meister, G., and Garlic, S., “CFD Application in Compact Engine Development”, SAE Paper 982016.

7. Ling, J. and Tun, L. T. Y., "CFD Analysis of Non-Symmetric Intake Manifold for Formula SAE Car", SAE Paper 2006-01-1976.
8. Jawad, B. A., Hoste, P. J., and Johnson, B. E., "Formula SAE Dual Plenum Induction System Design", SAE Paper 2002-01-0457.
9. Society of Automotive Engineers, "2006 Formula SAE Rules", http://www.sae.org/students/fsaerules.pdf (31 May 2006).
10. Blair, G. P. and Mackey, D. O., "Racing Engine Design Options Investigated by Engine Simulation", SAE Paper 2000-01-3546.
11. Ioannou, M., Gurney, D., and Downing, J., "The Application of Design of Experiments 1D Simulation to Create a Rapid Concept Optimization Tool for I4 Engines", SAE Paper 2005-01-0226.
12. Laney, B. C., Computational Gasdynamics. Cambidge, UK: Cambridge University Press. 1998.
13. Ricardo Software, "WAVE 7.1 User's Manual", 2006.
14. Ricardo Software, "VECTIS 3.8 User's Manual", 2006.
15. Launder, B. E. and Spalding, D. B., "The Numerical Computation of Turbulent Flow", Computer Methods in Applied Mechanics and Engineering, 1974, 3:269-289.
16. Casey, M. and Wintergerste, T. (Eds.). ERCOFTAC Special Interest Group on "Quality and Trust in Industrial CFD": Best Practice Guidelines Version 1. Brussels, Belgium: European Research Community on Flow, Turbulence and Combustion. 2000.
17. Chen, A., Lee, K. C., Yianneskis, M., and Ganti, G., "Velocity Characteristics of Steady Flow through a Straight Generic Inlet Port", International Journal for Numerical Methods in Fluids, 21:571-590.
18. Guizzetti, M. and Colombo, T. "Combined WAVE-VECTIS Simulation of an Intake Manifold of V6 PFI Gasoline Engine", http://www.ricardo.com/download/pdf/vectis_combined_wave_vectis.pdf (31 May 2006).
19. Roache, P. J., "Error Bars for CFD", AIAA 2003-408.
20. Roache, P. J., Verification and Validation in Computational Science and Engineering. Albuquerque, NM: Hermosa Publishers. 1998.
21. Roy, C. J., "Grid Convergence Error Analysis For Mixed-Order Numerical Schemes", AIAA 2001-2606.
22. Stern, F., Wilson, R. V., Coleman, H. W., and Paterson, E. G., "Verification and Validation of CFD Simulations", Iowa Institute of Hydraulic Research Report No. 407, 1999.
23. Simpson, R. L., "Two-Dimensional Turbulent Separated Flow", AGARDograph No. 287 Vol. 1 1985.
24. Miller, D. S., Internal Flow Systems: Design and Performance Prediction. Houston, TX: Gulf Publishing Company. 1990.
25. Smith, A. J. Ward, Pressure Losses in Ducted Flows, Butterworth, 1971.
26. Wyatt, D. D., "Analysis of Errors Introduced By Several Methods of Weighting Non-Uniform Duct Flow" NACA-TN-3400, 1955.
27. Pianko, M. and Wazelt, F., Suitable Averaging Techniques in Non-Uniform Internal Flow Propulsion and Energetics Panel Working Group 14, AGARD-AR-182, 1983.
28. Kobayashi, T. and Arase, K., "Intake System Optimization by Intake Loss Coefficient Method", SAE Paper 1999-01-3337.
29. Taylor III, W., Leylek, J. H., Sommer, R. G., and Jain,S. K., "IC Engine Intake Region Design Modification for Loss Reduction Based on CFD Methods", SAE Paper 981026.
30. Pan, W., Cui, Y., Leylek, J. H., Sommer, R. G., and Jain, S. K., "A CFD Study of Losses in a Straight-Six Diesel Engine", SAE Paper 1999-01-0230.

CONTACT

Mark R. Claywell has a Bachelor in Mechanical Engineering from the University of Minnesota. clay0052@umn.edu

Donald P. Horkheimer has a Bachelor in Aerospace Engineering and Mechanics from the University of Minnesota.hork0004@umn.edu
http://www.me.umn.edu/~hork0004

Garrett R. Stockburger has a Bachelor and Masters of Science in Mechanical Engineering from the University of Minnesota. stoc0086@umn.edu

DEFINITIONS, ACRONYMS, ABBREVIATIONS

AAD: Average Absolute Deviation

AFR: Air to Fuel Ratio

CAD: Computer Aided Design or Crank Angle Degrees

CAE: Computer Aided Engineering

CFD: Computational Fluid Dynamics

CSP: Conical-Spline Intake Concept

Concept: An abstract engineering idea that could conform to some if not all of the engineering specifications for a given application.

Design: A manifestation of the concept that conforms to all engineering specifications for a given application.

ECU: Engine Control Unit

GCI: Grid Convergence Index

ISE: Side Entry Intake Concept

PDE: Partial Differential Equation

RPM: Revolutions Per Minute

TF: Top/Center Feed Intake Concept

VE: Volumetric Efficiency

WOT: Wide Open Throttle

NOMENCLATURE

General

e_T	Internal Energy	[J]
E	Relative Error	-
F_s	Factor of Safety	-
k	Thermal Conductivity	[W/m*K]
K_c	Total Loss Coefficient	-
μ	Dynamic Viscosity	[Pa*s]
N	Number of Measurements	-
p	Order of Accuracy	-
P	Absolute Pressure	[Pa]
P_t	Total Pressure	[Pa]
r	Ratio of Grid Refinement	-
ρ	Density	[kg/m^3]
T	Absolute Temperature	[K]
u	Velocity	[m/s]
x_i	Individual Measurement	-
$\bar{x}$	Mean Value of Many Measurements	-

Subscripts

$_1$	Properties at Upstream Condition	-
$_2$	Properties at Downstream Condition	-